

Article

The Modern Nile Delta Continental Shelf, with an Evolving Record of Relict Deposits Displaced and Altered by Sediment Dynamics

Omran E. Frihy^{1,*} and Jean-Daniel Stanley^{2,*}¹ National Water Research Center, Coastal Research Institute, Alexandria 21514, Egypt² Mediterranean Basin (MEDIBA) Program, 6814 Shenandoah Court, Adamstown, MD 21710, USA

* Correspondence: frihyomr22@gmail.com (O.E.F.); stanleyjd0@gmail.com (J.-D.S.)

Abstract: The most extensive coverage of surficial sediment samples collected to date on Egypt's Nile Delta coast and shelf is needed to better define sediment dispersal patterns across this setting's rapidly eroding margin. Changes in time are now induced by River Nile sediment cutoff by dams, sea level rise, marked shelf subsidence, and regional climate changes, which have altered the amounts and components of sediments; these require replacement, along with the implementation of more effective coastal protection measures. Multiple computer-generated offshore maps depict the distributions and proportions of sand, silt, and mud; the mean grain size and standard deviation (sorting); heavy mineral concentrations; and carbonate content. Heavy mineral lobes at the coast and offshore identify former Nile branch sites. Channel lobes extending seaward resulted from their progradational phase and from the delta's altered sedimentation from the early to late Holocene. The progressive deposition and erosion of these fossil fluvial lobes, and of two active Nile channels, selectively removed their quartz and less dense minerals, thus concentrating heavy minerals on the coast and inner shelf. The prolonged dispersal of original sediment effluence from relict and recent Nile tributaries induced variable depositional patterns on the present shelf. These coastal depocenters, along with extensive sand, silt, and mud from shelf sediments, were reworked further seaward and dispersed by bottom currents, thus masking most previous onshore-to-offshore transport patterns. The major surficial features document long-term responses to the diverse dispersal that influenced the shoreline to the outer shelf deposits from the Pleistocene to the present.

Keywords: abandoned estuaries; carbonate ridges; coastal sedimentation; erosional processes; fluvial lobes; heavy minerals; nearshore depocenters; sand belts; seabed dynamics; shoreline phases



Citation: Frihy, O.E.; Stanley, J.-D. The Modern Nile Delta Continental Shelf, with an Evolving Record of Relict Deposits Displaced and Altered by Sediment Dynamics. *Geographies* **2023**, *3*, 416–445. <https://doi.org/10.3390/geographies3030022>

Academic Editor: Karoly Nemeth

Received: 12 March 2023

Revised: 6 June 2023

Accepted: 13 June 2023

Published: 21 June 2023



Copyright: © 2023 by the authors. Licensee MDPI, Basel, Switzerland. This article is an open access article distributed under the terms and conditions of the Creative Commons Attribution (CC BY) license (<https://creativecommons.org/licenses/by/4.0/>).

1. Introduction

Large fluvial deltas bordering marine settings are generally envisioned as major sedimentological units developed primarily on land, which extend to the coast. In fact, a large or greater portion of their integral deposits can extend well offshore, even beyond their continental shelves and all the way to distal deep seafloors. Many studies of Egypt's Nile Delta on land have called attention to the changes induced before and since the Holocene that have occurred via both natural and anthropogenic means. There have been far fewer comprehensive analyses of the changes that have taken place below sea level during this period. The current study focuses on the offshore section of this delta, with the aim to detail its Holocene to present evolution. The River Nile, the world's longest fluvial system, has been identified as a major source of siliciclastic sand, mud, and heavy minerals on the coast and its adjacent continental margin [1,2]. The Nile Delta is recognized as the major source of Nile deposits on Egypt's northern coast and its contiguous continental margin (Figure 1). These latter settings have been seriously affected also by the Aswan High Dam in Southern Egypt, which has entrapped a large proportion of its sediment and experienced a considerable amount of evaporation of its water in its elongate Lake Nasser

reservoir since its emplacement in 1964–1965, where a new Nile Delta is now forming. This dam, the two dams on the still active major distributaries landward of the coast, and the new GERD Dam in Ethiopia, now the largest in Africa (closed in 2022), prevent the bulk of sediment and much freshwater transport from displacement to and beyond the present coast as in times past.

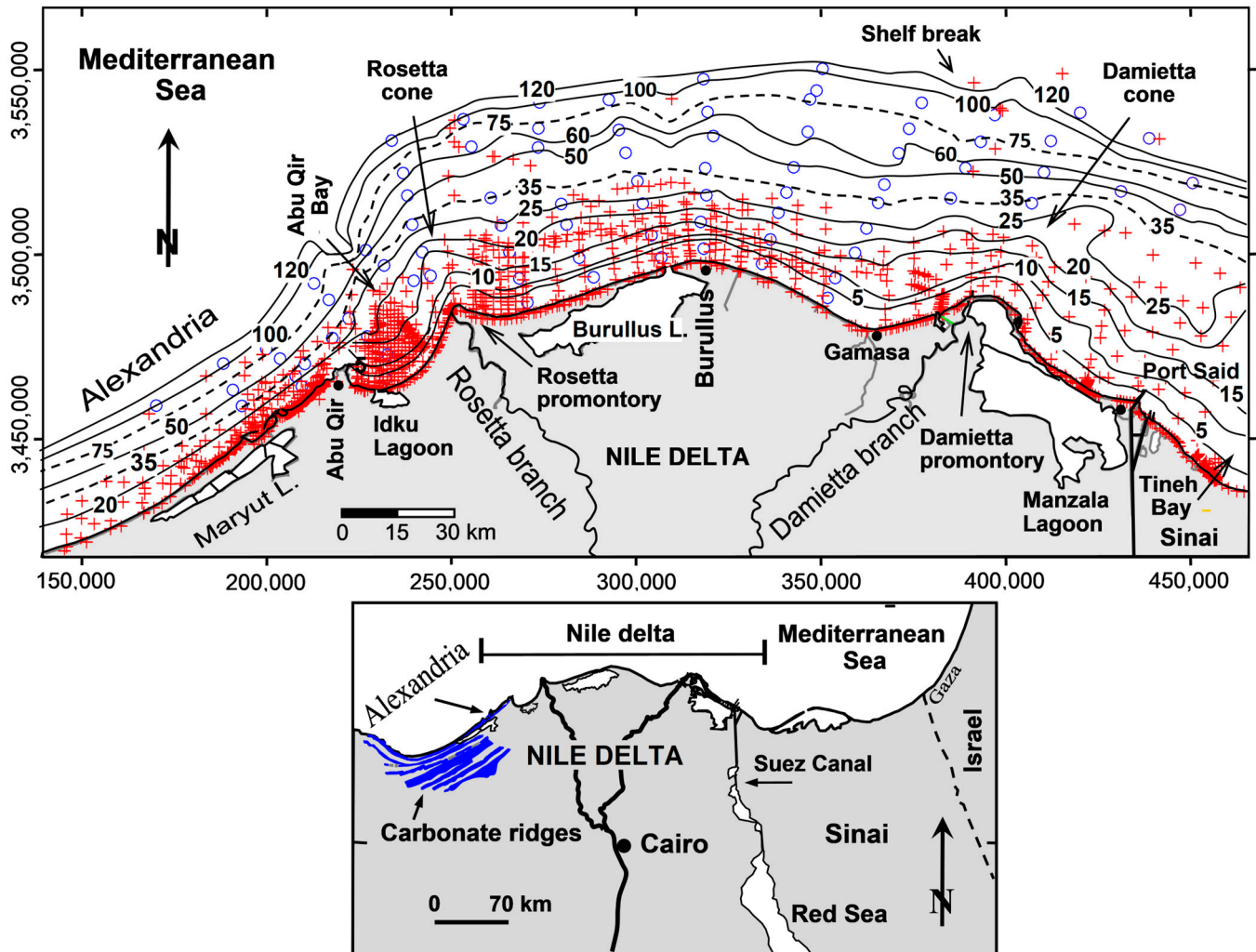


Figure 1. Alexandria–Nile Delta continental shelf extending to the north of Tineh Bay. Map shows the location of examined surficial sample stations recovered by Woods Hole Oceanographic Institution, USA (blue circle symbols) and Coastal Research Institute (CoRI) of Egypt (red cross symbols and pink in dense sampling areas). Also shown are positions of the presently active Rosetta and Damietta Nile branches. Bathymetry (depth in meters) generated in this study is depicted on the delta shelf. The lower map shows configuration of linear coast-parallel limestone ridges on the backshore of Alexandria [3,4]. Map coordinates are in Universal Transverse Mercator (UTM).

Seasonal floods have now stopped the natural cycle of sediment infill along the delta’s offshore marine margin. This much-diminished seaward sediment transport makes the coast and offshore region more vulnerable due to increased erosion and apparent saltwater intrusion. This decrease in available essential freshwater for human consumption and farmland production in the northern delta is amply indicated by the current pumping up to the delta surface of saline groundwater. A primary purpose of this study is to establish a recent measure of the delta’s offshore setting that can be used as an increased database anchor to comprehensively identify and help to track future changes after more than a half century of these Nile water and sediment depletions. Study of this sediment

entrapment and displacement is also needed to provide a basis to guide more effective coastal protection engineering projects, which are increasingly needed as sedimentation patterns and fresh water supplies continue at present [5]. This is significant, especially now, with Egypt's total population having reached approximately 102 million and with 50 million now concentrated in the Nile Delta, from Cairo at the southern delta axis to its northern arcuate coast. This comprises an area along the southern Levantine basin of approximately 22,000 km², which accounts for only approximately 3% of Egypt's total land area.

Previous reconnaissance studies of Alexandria shelf sediments were carried out by El Sayed [6] and El Wakeel and El Sayed [7], and those off the more central delta were studied by El Wakeel et al. [8]. The previous lack of sufficient shore-to-middle shelf samples, leaving large gaps between sampling stations that characterized earlier reconnaissance studies, made it difficult to provide answers to a number of questions that have been raised. These include the selection of sufficient locations of coarse-grained sand resources for beach nourishment and the mining of heavy mineral placers. Additionally needed are determinations of land-to-marine stratigraphic connections and an evaluation of the types and degree of stability of bottom sediments for coastal protection measures and for increased delta population and industries such as gas and oil production, as well as their effects on subsidence and the tectonic displacement of bottom sediments.

The numerous, closely spaced samples in the present study (Figure 1) include a database of 1747 beach and bottom surficial grab samples and short cores. These can now better serve to fill missing data gaps along the shore and inner shelf that existed in previous surveys of the Alexandria–Nile Delta continental shelf, and thus provide a much-needed detailed, updated numerical base. The updates presented herein, based on a now much larger sample database, focus primarily on refining the sediment texture and heavy mineral concentrations along the coast and on the continental shelf off the delta's land sector. These allow the better definition of the offshore positions of remnant estuaries of the delta's extinct fluvial Nile branches that once reached the sea, and provide a means to further interpret Holocene to present offshore sediment erosion, displacement and transport dynamics, and regional redepositional patterns.

2. Physical Settings and Background

The continental shelf is ~20 km wide near Alexandria and widens to ~45 km off the Rosetta promontory, and then to a maximum of ~75 km off the north–central delta. The delta is bordered by a ~305-km-long shoreline extending from Alexandria in the west to off the northwestern Sinai in the east (Figure 1). Excluding harbors, the rocky shores of Alexandria (65 km long) are mostly covered by a thin veneer of carbonate sand that is locally derived from the erosion of beach and ubiquitous bedrock outcrops [3,4,7–9]. The city of Alexandria is built on the second carbonate ridge, called Abu Sir, that reaches a height of 35 m in its western part and 6 m near Abu Qir. Some small western branches of the Nile once reached waterways in this area. The carbonate components of Alexandria consist mainly of bioclastic, pelletal carbonate sands and muds. In contrast, the extensive and, for the most part, low-lying shoreline (~240 km long) from the Abu Qir headland to 25 km east of Port Said off the northwest Sinai comprises gently sloping, siliciclastic sandy beaches interrupted by two modern promontories located at the mouths of the Rosetta and Damietta Nile channels. An intermediate relict and now rounded, highly eroded bulge at the Burullus headland (Figure 1) was originally formed by the ancient Sebennitic Nile branch (Figure 2). The sandy beaches are backed partially by the low-lying delta coastal plain, dunes, cultivated land, residential centers, and brackish water lagoons (Idku, Burullus, and Manzala). These are separated from the sea by sandy barriers breached by artificially protected inlets. In addition, the brackish Maryut Lagoon, disconnected from the sea, is located southeast of Alexandria.

Hydrodynamically, the coarse-grained and relatively steep coast to offshore slope, and the narrow surf zone at Alexandria's beaches where waves break close to shore, are

classified as reflective beaches (1:30). In contrast, at most of the Nile Delta sectors to the east, the relatively fine-grained, siliciclastic beaches allow waves to break and dissipate their energy across a wider, smoothed, and gentler nearshore slope (1:50 to 1:100) [10]. The depth of the shelf area is divided topographically by Misdorp and Sestini, 1976 [11] into the (I) inner (0–36 m), (II) middle (36–75 m), and (III) outer shelf slope (75 m—outer shelf break) sectors, and morphologically into the ridge zone (A) and upper (B) and lower (C) terraces (Figure 2). These latter are separated by coastal (I), middle (II), and outer (III) shelf slopes. Previous studies have indicated that sediments on the inner shelf are mostly recent, predominantly terrigenous sand with fauna of recent age, whereas, on the outer shelf, they tend to be reworked and relict (palimpsest) deposits composed of calcareous bryozoans with coralline algae and carbonate mud. An admixture of reworked terrigenous and biogenic sand and pro-delta mud dominates the middle shelf.

Despite the sparser sampling on parts of the Nile Delta shelf, particularly in the area to the north of Manzala Lagoon and to the east of Port Said, the general distribution of the seabed sedimentary facies and their evolution has been documented by Summerhayes et al. [12], Frihy and Gamai [13], and Stanley and Bernasconi [14]. These studies indicate that the sedimentation patterns on the Nile Delta continental shelf are the result of the dispersal of the annual Nile flood water and its sediments which, over time, have been effluent from at least seven former distributary channels that flowed across the Nile Delta and discharged into the Mediterranean during earlier Holocene phases of the delta's evolution [2,15,16]. These branches are the Canopic, Saitic, Sebennitic, Athribic, Mendesian, Tanitic, and Pelusiac. Over time, and as a result of major episodic physical interventions, including the lowering of the northern delta and shelf by subsidence and tectonic offset, these seven distributary channels became silted over, whereas another two, the present-day Rosetta and Damietta branches, remain partially active even after the closure of the Aswan High Dam in 1964–1965 [2] and the two dams (barrages) in the northern delta placed behind the mouths of the Rosetta and Damietta branches. When the relict branches were active, they likely formed promontories, some with estuaries similar to those that have developed at the mouths of the Nile's present-day Rosetta and Damietta distributary channels. The locations and general positions of these former distributary channels on the delta plain, together with the present, partially active Rosetta and Damietta branches, are shown in Figure 2.

Heavy minerals on land and in the littoral zone have already attracted attention and interest for research related to their economic importance and processes of formation. There is much less information on heavy minerals recovered in the inner shelf sediments off the Nile Delta. On the delta, heavy minerals (density $\rho_s = 5.3 \text{ g/cm}^3$) are commonly concentrated in the finer sieved fractions of fine sand, very fine sand, and coarse silt. These minerals include mainly hornblende, augite, ilmenite, zircon, garnet, magnetite, rutile, and monazite. In contrast, among the mineralogical components are light minerals, which primarily comprise quartz and lesser amounts of feldspars and organic shell fragments. Previous studies have confirmed that the hydrodynamic processes of waves and currents play a significant role in the grain-sorting processes and concentrations of heavy minerals in beach and surf-zone sediments. The major heavy mineral concentrations dominate areas of shoreline erosion away from their coastal input sources, mostly at promontory margins. These also decrease progressively with longshore distance, toward areas where there has been beach accretion [17]. Heavy minerals thus prove to be one of the most useful components in the present study.

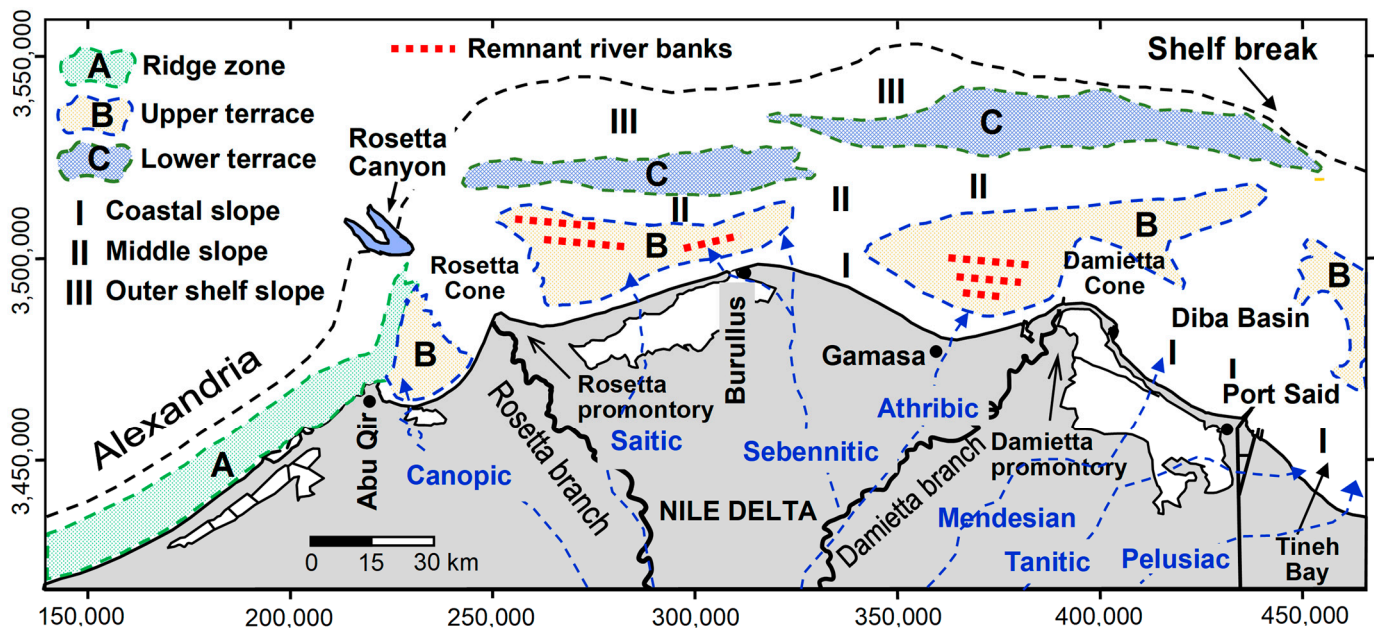


Figure 2. Major topographic features on the study continental shelf: (A) ridge zone, (B) upper terrace, and (C) lower terrace, separated by (I) coastal slope, (II) middle slope, and (III) outer shelf slope (modified after Misdorp and Sestini, 1976) [11]. Also shown are traces of seven former north-trending distributary channels landward of the coastline (dashed lines), now submerged (after Toussoun, 1922 [15]; Said, 1981 [2]) and the two still-active channels of the Rosetta and Damietta branches (solid lines). Positions of buried alluvial banks of the former Nile branches that were identified as sources of the beach pebbles are shown by red dots [11]. Map coordinates are in Universal Transverse Mercator (UTM).

The processes of alternating erosion and accretion along the delta coastline induced a concentration of heavy minerals on stretches along the shifting shorelines, close to where they originated, whereas light minerals were selectively moved further away toward accretion areas. Thus, denser minerals tend to remain as pod-shaped lag concentrations in eroding high-energy sectors (Figure 3). In nature, this operation takes place through what is called ‘grain-sorting processes’. Waves and currents sort and concentrate the heavy mineral grains according to their densities, sizes, and shapes during the transport of sand between eroding and accreting shores [18,19]. As such, heavy minerals in the Nile Delta’s coastal/nearshore zone have been widely used as natural tracers of sand transport related to shoreline and seabed change. In the same context, and at a local to wide scale, multiple lines of work have been undertaken to trace the positions of some of the former channels of the Nile in different environments, including the northern delta plain, beach, and nearshore zone. In the latter, for example, heavy minerals are used to locally refine the position of the Sebennitic promontory off the central bulge of the Burullus coast. On a delta-beach scale, the former Canopic mouth to the west of Abu Qir Bay was traced by El Bouseily and Frihy [20] and the Sebennitic by Frihy [17]. Heavy minerals were also used to define five other sediment transport sub-cells along the delta’s coastal/nearshore zone.

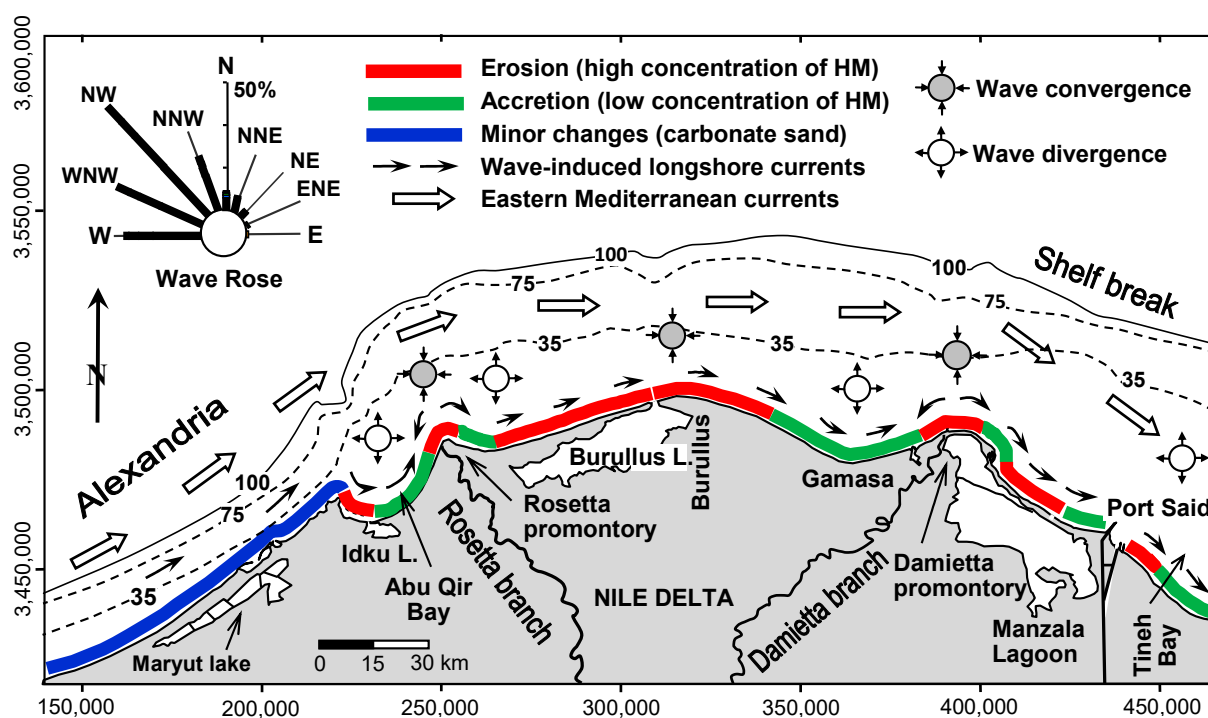


Figure 3. The Alexandria–Nile Delta coastline shows schematically an along-shore erosion and accretion pattern [21] and the dominant dynamic system along the coast and shelf area. This system includes prevailing longshore sediment transport paths (small arrows) induced by wave-driven and eastern Mediterranean currents [22,23]. Reversibility of easterly and westerly driven longshore currents results in response to change in wave direction from NW and NE quadrants relative to shoreline orientation. Wave convergence (high energy) and divergence areas (low energy) are inferred from wave refraction patterns [24]. Heavy minerals (HM) are highly concentrated within wave convergence areas and diluted towards wave divergence zones [17]. Shown also in the upper part of the figure are wave rose and dominant wave components (after Frihy et al., 2021 [25]). Map coordinates are in Universal Transverse Mercator (UTM).

Unlike heavy minerals, other work also has been undertaken to identify the former estuary positions where the Nile branches reached the sea. On the delta plain, the path of the buried Canopic branch was traced using magnetic indications [26], Radar (SRTM) imagery [27], high-resolution seismic data, and short vibro-cores [28]. The Sebennitic and associated smaller distributaries that form the north–central deltaic Burullus bulge were mapped via satellite imagery and sediment cores drilled south of the present coast [29]. In addition, a number of now-extinct Nile distributary channels and delta lobes (Mendesian and Pelusiac) and the overbank deposits (Sebennitic) were interpreted in the delta plain from the petrologic analyses of numerous radiocarbon-dated core samples located landward of the present coastline [30,31]. The inland delta traces of these buried Nile branches are shown in Figure 2.

3. Interpreting Sediment Dispersal

The cross-shore movement of energy-level sediment transport inferred from the grain size distribution of shelf sediments and the proportions of heavy mineral concentrations have long been used to determine the depth of closure and the sand–mud line. The concept of the depth of closure is based on the observation that cross-shore sediment transport tends to decrease seaward. The depth at which its effect on the seabed morphology and composition becomes almost negligible beyond a certain depth is identified as the closure depth [32]. This depth is an offshore location with minimum heavy mineral concentrations that record where there has been a decrease in energy levels on the seabed. Distinct changes

in sediment attributes (texture, color, heavy minerals, and/or benthic faunas, for example) along shore-normal profiles have been used as geological indicators to help to identify and delineate the depth of closure [33]. Off Alexandria, for example, the position of the offshore boundary separating recent non-stained sand from relict stained sand facies is used to define the depth of closure there, usually between 8 and 10 m.

The sand–mud line is identified where the transition from sand to mud occurs. This can be identified at the sector of the seafloor where the mass percentage of grains with diameters of less than 63 μm (upper limit of silt) in the sediment increases rapidly, and it generally corresponds to the boundary between prevailing erosion and deposition [34]. Locally, on the northwest coast of the Nile Delta, a depth of closure between 20 and 24 m was determined from the analysis of historical bathymetric maps surveyed in 1920, 1976, and 1984 [35].

One of the objectives of the present study is to trace, where possible, the aerial extent of textural attributes of the original sediment and those of heavy mineral concentrations based on newly available, closely spaced sample compilations from beaches and seaward sectors onto the continental shelf of the Alexandria–Nile Delta sector. This denser, closely spaced coverage of sample analyses could perhaps address previous sampling gaps that existed in earlier studies. The computer-generated maps of heavy mineral concentrations and sediment depositional texture patterns on the study shelf are used here to achieve the following: (1) locating traces of earlier Nile Delta channel estuaries and their relations to Nile Delta depositional phases during the early Holocene to the present time, as influenced by changing eustatic sea level positions and delta plain and offshore subsidence; (2) updating and refining the mineralogical and textural characteristics of the shelf sediments with the objective of the better identification of processes of hydraulic grain-sorting patterns; these could help to refine provenance-to-depositional patterns and thus allow us to better infer sediment transport processes that could be validated with previously published hydrodynamic observations; and (3) delineating and refining positions recording long-term energy and depositional zones across the uneven surface of this shelf area.

4. General Coastal and Shelf Dynamics

In the study area, beach and nearshore sediments are moved and reworked by two inter-related transport mechanisms: longshore and coastal currents [36,37]. The longshore or littoral currents are most intense in and near the surf zone and are primarily generated by wind-driven waves approaching the coastline at oblique angles. The longshore currents derive primarily from the NW quadrant and seasonally from the NE. On a delta-wide scale and depending on the shoreline orientation versus wave direction, the longshore current flow is almost unidirectional to the east all year, with a minor episodic westward reversal (primarily driven from the NE) but with a net flow to the east, as shown in Figure 3 (Fanos et al., 1991 [21]). Further offshore, these wave-induced longshore currents are combined effectively with the dominant counter-clockwise geostrophic East Mediterranean current that extends to and operates on the middle and outer shelf [22,23]. Occasionally, during periods of storm waves, this easterly flowing Mediterranean gyre can move sand further to depths of 40 m [37,38]. On the other hand, the seasonal reversal in the direction of waves, combined with the shoreline orientation at the Alexandria margin that normally trends SW-NE, can produce locally reversed longshore currents. Nevertheless, they drift littorally toward the east when currents are averaged over several years, as shown in Figure 3 (after Frihy et al., 2021 [25]). Tidal variation in the study area follows a semi-diurnal micro-tidal regime with a maximum tidal range of ~50 cm [39]. Accordingly, this smaller tidal range does not allow the formation of significant tidal currents.

Levels of wave energy along the delta coast, modeled by Quellenec and Manohar [24], take into account the refraction of waves derived from the prevailing NNW direction. High-wave-energy convergence orthogonals are prominent at the Rosetta, Damietta, and Burullus promontories and are directed to both the east and west by low-wave-energy divergence along concave coastlines that exist immediately on both sides of these promon-

tories (Figure 3). Overall, there are periodic reversals in wave direction and energy from NW to NE quadrants; these are noted on the wave rose diagram in Figure 3. They result in alternating erosion along high-energy sectors and accretion zones at low-energy beaches.

5. Delta Shoreline Displacement Phases to the Present

The geological evolution of the Nile Delta's shoreline during the Holocene can be divided into three delta shoreline phases, coded I to III (Figure 4). These three phases are used in this study as a basis to help to interpret the origins of the identified depositional shelf sediments. These phases are proposed based on results obtained from the delta shelf sediments [12] and from core logs drilled south of the present coastline [40,41]. The migratory trends of these shoreline phases landward to the south (sea transgression) or to the north (sea regression) are indicated by arrows in Figure 4. During the first phase (I), an extensive coastline retreat landward, locally to as much as 30 km south of the present eastern delta shoreline across the shelf, reached what is now the subaerial, low-elevation alluvial delta plain during the late Pleistocene to the early Holocene. This occurred during a period when the sea level rose rapidly and migrated landward, as shown by the blue long arrows in Figure 4b.

The continued reworking and landward displacement of deposits across both the former shelf and alluvial plain deposits formed shallow marine or nearshore sands, known as 'transgressive sands' (Figure 4b). The original morphologies of the Nile Delta estuaries, including those considered in this study, were significantly modified as they shifted seaward during the progradational phase (II) of the Nile Delta from the early to mid-Holocene to the early part of the late Holocene sea regression from ~7500 to ~3000–2000 yr BP (Figure 4c, solid dark arrows depict seaward coastline displacement in phase II). During this phase, the delta lobes, formed from delta-front and prodelta deposits up to ~50 m in thickness, prograded and were deposited further seaward of the mouths of now-abandoned distributary channels (Figure 4c). This occurred on what are now submerged inner continental shelf sectors to a depth of 20 m, which corresponds to ~10 to 25 km distances northward of the present-day delta coast. This progradational phase II was controlled by the effects of fluvial sediment input from numerous relict Nile branches that flowed to the coast during low-sea-level stands from ~10 mm/yr to 1–2 mm/yr. It is of note that the fluvial sediment input to the Mediterranean accounted for as much as 134 million tons/year before the construction of the High Aswan Dam, which began filling in 1964 [42]. The closure of the GERD dam in Ethiopia in 2022, the largest in Africa, is now further reducing the amount of Blue Nile water flowing to Egypt, its delta and coast, and offshore sectors. It is now vital that work on the coast and offshore in the study area be performed to evaluate its effects.

Subsequently, in the late Holocene to the present time (~3000–2000 yr BP to now), the former delta lobes retreated landward, as a result of sea transgression, from their original position at the inner shelf (~20 m water depth) to the present-day arc-shaped erosional coastline (phase III, small blue arrows depicting this phase in Figure 4d). This phase has been triggered by the relative sea level rise (1.7 mm/yr–3.0 mm/yr) and shore erosion responding to northern delta plain and offshore subsidence, much of which has affected the presently still active Rosetta and Damietta promontories [41]. The erosional processes dominating in this phase effectively accelerated the formation of heavy mineral concentrations at eroded former estuaries, an observation noted in the present study. In addition, some former Nile tributaries were reduced or even ceased to flow during this marked arid to desert climate change, which began to markedly intensify in Lower Egypt approximately 4000 years ago [43]. Exceptions were those of the two now still partially active, but much reduced flow of Rosetta and Damietta channels after the High Dam's construction.

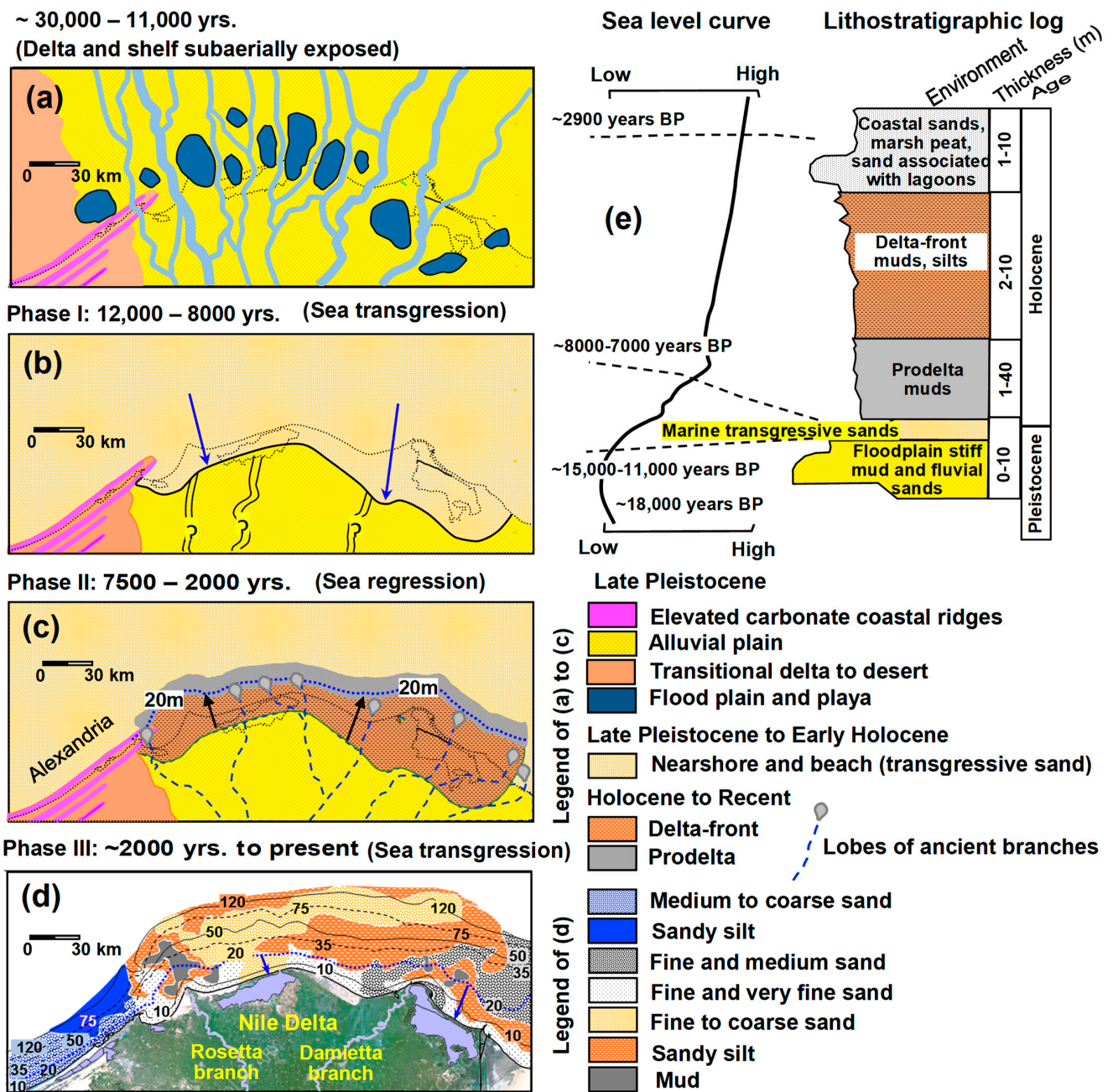


Figure 4. Time-slice paleogeographic maps detailing the evolution of the northern Nile Delta from the late Pleistocene to the present. (a) Delta and shelf subaerially exposed, (b–d) the three depositional phases during the delta’s shoreline evolution from the late Pleistocene to the present time (modified after Stanley and Warne, 1998 [44]; Stanley and Clemente, 2014) [41]. (b) Phase I: landward retreat southward across the shelf area in the late Pleistocene to early Holocene. (c) Phase II: shoreline seaward advance northward up to the ~20 m depth contour, where the estuary deltaic lobes of the former distributary channels formed during the mid–late Holocene, interpreted in this study. (d) Phase III: return landward of the coastline during late Holocene from the present inner shelf, now submerged. Heavy mineral deposits displaced during this phase are one of the subjects of this study. (e) A composite simplified lithostratigraphic log representing the eastern delta margin, depicting the late Pleistocene and Holocene sequences (modified after Stanley et al., 1992 [45]).

6. Materials and Methods

The sediment texture and heavy mineral concentrations examined in this study were analyzed from selected beach and surficial grab samples collected on the delta shelf. Surficial samples considered here were collected during Chain Cruise 119 in 1975 ($n = 83$ samples). In addition, a number of beach ($n = 247$) and seafloor shelf samples ($n = 1417$) were also collected during a systematic sampling program conducted in 2010–2014 through the STDF joint project (Science and Technology Development Fund), funded by the Academy of Scientific Research and Technology and the Coastal Research Institute (CoRI) in Egypt. The closely spaced positions of all now-merged samples (1747) (Figure 1) allows the filling of gaps that existed in previous studies and also facilitates a regional comparison/correlation between the fluvio-marine deltaic settings of the Nile Delta and the marine carbonate environments that prevail off Alexandria. Grain size analysis was performed first via the wet separation of the sand and mud (silt and clay) using a 63 μm sieve. The sand fraction was analyzed by dry sieving, while the fine fraction was analyzed using the pipetting procedure of Folk (1974) [46]. Grain size determination was performed according to phi (ϕ) scale intervals after Krumbein (1934) [47]. Commonly used grain size parameters were determined for each sample using the formulae of Folk and Ward [48]. These were the graphic mean grain size (M_z) and the graphic standard deviation (σ_1), both in phi (ϕ) units (Table 1).

Table 1. Main textural results of the identified sedimentary zones.

Sedimentary Zones		Mean Grain Size M_z (ϕ)	Sorting (ϕ)	Textural Description
Alexandria (Carbonate)	Coastal to shelf	1–2	0.35–0.50	Medium sand, moderately well sorted (SW trend)
		4–6	0.7–1.0	Sandy silt, moderately sorted (NE trend)
Nile Delta (Siliciclastic)	W-to-E coastal sector	2–4	0.5–1.0	Fine to very fine sand, moderately well sorted to moderately sorted, with small patches of medium to coarse sand ($M_z = 0.0\text{--}2.0 \phi$; $\sigma_1 = 0.5\text{--}1.0 \phi$)
	Mud-rich linear and mid-shelf	5–8	1.0–1.5	Silt, poorly sorted bordered by poorly sorted sandy silt ($M_z = 4\text{--}7 \phi$; $\sigma_1 = 1.0\text{--}2.0 \phi$)
	Belt 1	0.0–3.0	1.0–3.0	Fine to coarse sand, very poorly sorted
	Belt 2	1.0–3.0	0.8–1.4	Fine-to-medium sands, moderately to poorly sorted
	Belt 3	4.0–7.0	1.0–2.0	Sandy silt, poorly sorted

Heavy mineral separation was conducted for 553 selected samples that contained an appreciable amount of heavy minerals. In these samples, the 3 ϕ (125 μm) to 5 ϕ (31 μm) grain size range was separated from the light minerals by using bromoform with a specific gravity of 2.89 via a set of separation funnels. The petrologic composition of the coarse sediment fraction ($>4 \phi$) in the examined depositional features was obtained from the studies of Summerhayes et al. (1978) [12] and Frihy and Gamai (1991) [13]. In addition, the carbonate content in 529 representative samples was determined by gasometric analysis. The primary database used in the present study included the total relative percentages of sand, mud, carbonate content, and heavy mineral concentration, as well as the mean grain size and sorting of grains. These data, along with extensive depth-sounding profiles (513,491 data points), were utilized to generate high-resolution contour maps via the linear interpolation triangulation method in the Surfer software, version 16. Data and maps were geographically coordinated according to the Universal Transverse Mercator (UTM) metric system, Zones 35 and 36, and the World Geodetic System (WGS 84). The generated maps are discussed here with aid of the shelf morphology and the major depth boundaries (inner, middle, and outer shelf) defined by Misdorp and Sestini [11].

7. Four Regional Depositional Trends

The spatial patterns of the sand and mud percentages of sediments at and along the study coast and on the more open shelf areas show four major distributions, presented in

Figures 5 and 6. These depositional sectors between the coast and the outer shelf to the shelf break at ~120 m depth are identified as follows: (1) the western carbonate-rich coastal and shelf sectors off Alexandria to Abu Qir; (2) coastal and inner shelf sectors where former and modern Nile distributaries at and near their mouths released siliciclastic deposits at and near former and present shorelines, including those found locally that tend to be enriched with heavy minerals, as seen in Figure 4c; (3) small to moderately sized, often linear, mud-rich zones isolated on the shelf proper—two of these are small and narrow and trend in a linear fashion northwest of the Rosetta cone and northeast of the Damietta cone (Figure 7), the two present still-active Nile distributaries extending onto the shelf proper, and one larger one trending generally west–east on the mid–central shelf (Figure 5b); and (4) three major, large, elongate curvilinear sand and sandy silt belts on the open shelf proper, extending from the north of Abu Qir to the north of the Gulf of Tineh (Figure 7). Data on currents measured in different sectors of the coast to outer shelf and beyond of the study area are provided in Table 2.

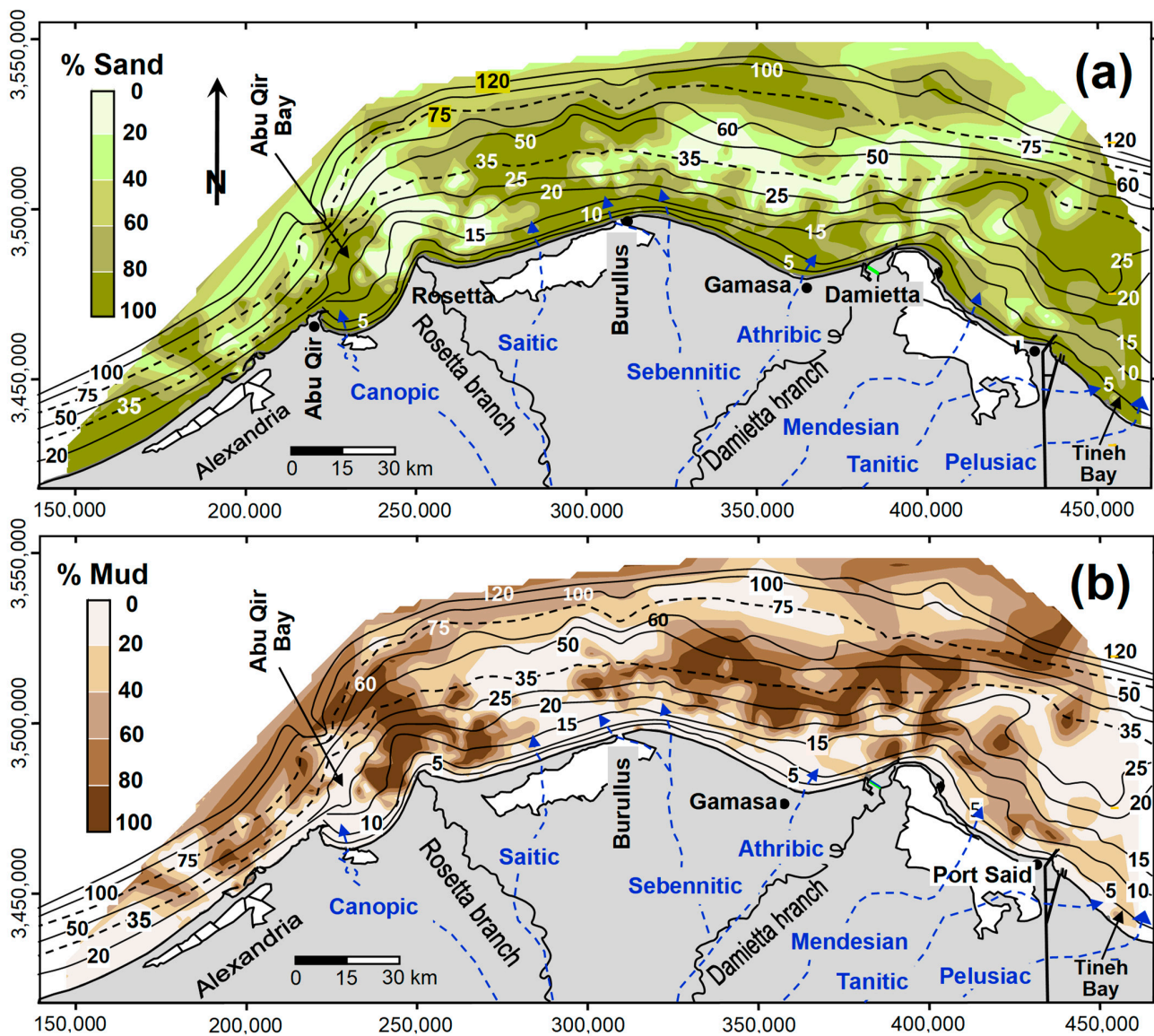


Figure 5. Spatial distributions of proportions of sand (a) and mud (b) in sediments of the beaches and shelves of Alexandria and wider Nile Delta. Water depth in meters. The dashed contour lines offshore indicate boundaries of the inner, middle, and outer shelf zones. Map coordinates are in Universal Transverse Mercator (UTM).

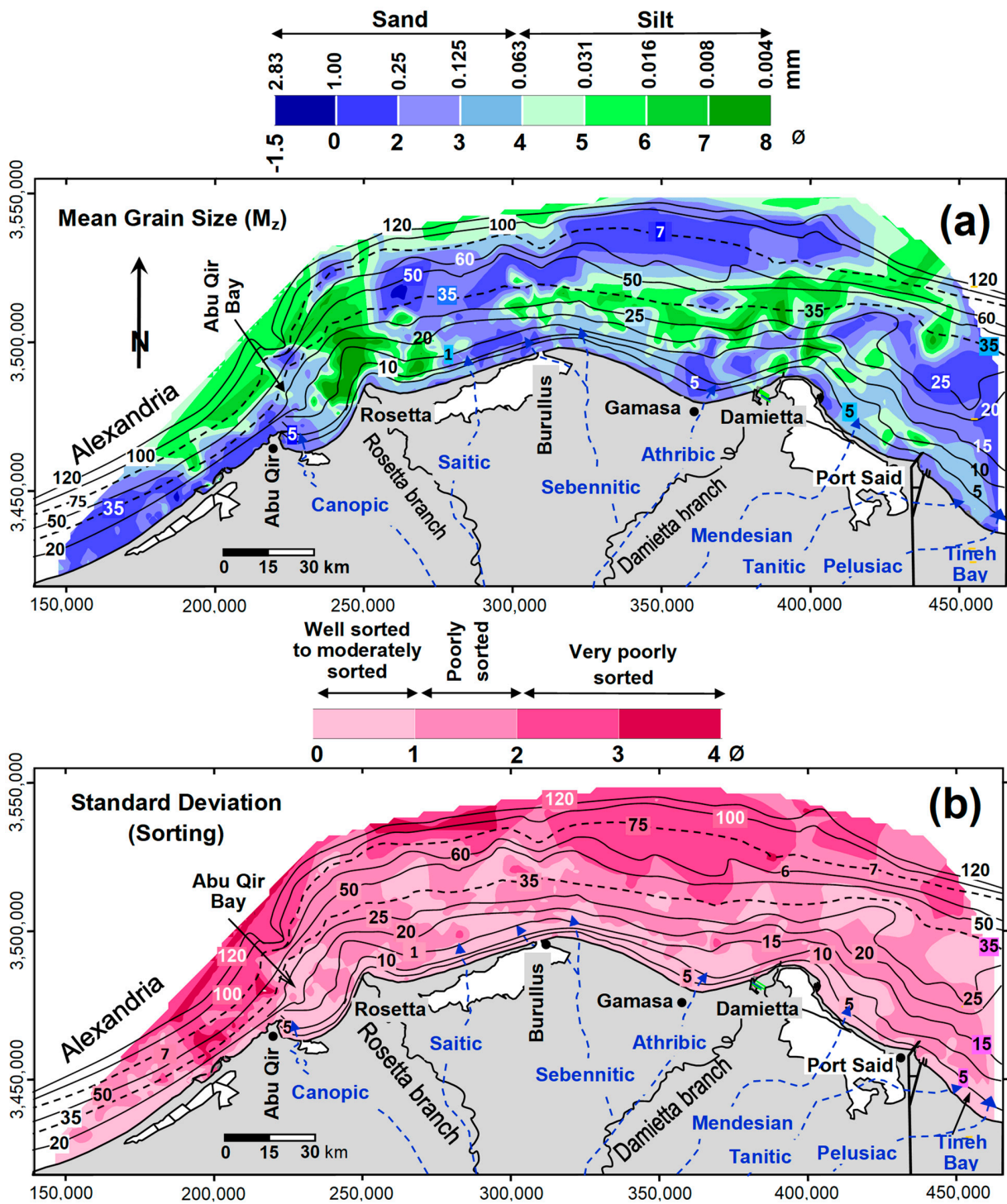


Figure 6. Spatial distribution of mean grain size (a) and sorting (b) of sediments in the coastal sector and shelf off the Alexandria–Nile Delta. Water depth in meters. Dashed contour lines separate boundaries of the inner, middle, and outer shelf zones. Map coordinates are in Universal Transverse Mercator (UTM).

Table 2. Bottom current data recorded between the coast (I) and shelf break (VII) at the seven areas examined in the study, in the Alexandria–Nile shelf.

References and Data Sources	Sedimentary Zones	Water Depth (m)	Velocity (cm/s)		Dominant Direction of Flow	Weather during Survey
			(Min–Max)	Average		
Frihy et al. (2010) [49]; * CoRI	(I) Alexandria’s carbonate coastal to shelf sectors	1.5–15	7–30	21	NE	Throughout most of the year
* CoRI	(II) Nearshore coastal sectors, including off Nile Delta distributaries	1.5–11.5	12–46	25	E-NE	Throughout most of the year
Tebelius (1977) [50]	(III) Linear mud sectors and mud extensions seaward offshore	12	3–11	6	NE-NNE	Non-winter weather
Said (1990) [51]	(IV) Belt 1	42–63	13.7–37.6	-	SSE-SSE	Winter storm
* Pc; Murray et al. (1981) [52]	(V) Belt 2	29–28	7–60	-	NE-E	Non-winter weather
Said (1990) [51]	(VI) Belt 3	27	37	-	ESE	Winter storm
Said (1990) [51]	(VII) Outer shelf	125–400	68–113	-	NE	Winter storm

* CoRI = Coastal Research Institute, Egypt, Alexandria; * Pc = personal communication with. Ebtessam El Sayed, Institute of Oceanography and Fisheries, Egypt.

7.1. Alexandria’s Carbonate Coastal to Shelf Sector

Former smaller Nile channels extended northwestward of the major Canopic branch and reached the enclosed waterways in Alexandria’s deltaic area, as noted by Flaux et al. [53] and Trampier [54]. Of note are the high proportions of sand in the relatively steep sloping carbonate ridge zone of the Alexandria shelf, which includes well-sorted medium sands (>90%) on the western shelf sector and moderately sorted sandy silt (>30%) on the NE middle and outer shelf areas (Figures 5a and 6a,b). The sand-sized grains on the beach and parts of the shelf zone in this area are composed largely of oolitic and pelletoidal sands (Stoffers and Summerhayes, 1980 [55]), primarily derived from the coastal limestone ridges extending to and across Alexandria’s seafront and eastward toward Abu Qir (Figure 1, lower map). According to the basic sorting mechanism, sediments move in the direction where the average grain size decreases (trending finer) and the sorting value increases, i.e., becoming better sorted. The dispersal fining trend of the mean grain size, from medium sands to sandy silts on the middle and outer shelf, indicates the net sediment transport of carbonate-rich deposits in an NE-trending direction. This is consistent with measured offshore current patterns at Alexandria to the NE, with a minor localized reversal recorded to the SW [49]. Despite Alexandria being classified as a high-energy refracting nearshore environment, the limestone ridges blanketing the seafront marine floor serve to dissipate considerable wave energy before it reaches the coast. Thus, ridges here provide a natural protection buffer for the coast as compared to long east-trending siliciclastic coasts of the delta farther to the east, which are without such solid cemented coast-parallel seafloor features [49,56].

7.2. Elongate West-to-East-Trending Coastal Sectors

Long belts parallel to the coast cover the more easterly oriented inner delta shelf and cover extensive seafloor areas with much higher proportions of siliciclastic sand, unlike the largely carbonate seafloor sediments west of Abu Qir (Figure 5a,b). In contrast to the SW-to-NE-trending Alexandria sector, the gently sloping quartz sand-rich zone (to >90%) covers much of the entire, more open, W-to-E-oriented delta coastal sector along most of the inner shelf and its coastal slope all the way from Abu Qir Bay eastward to the eastern end of the delta at the Gulf of Tineh (Figure 5a). This shallow and gently sloping

coastal-inner shelf sector is characterized by fine to very fine, moderately well-sorted to moderately sorted sands ($M_z = 2-4 \phi$; $\sigma_1 = 0.5-1.0 \phi$), with small areas consisting of medium to coarse sand ($M_z = 0.0-2.0 \phi$; $\sigma_1 = 0.5-1.0 \phi$), as seen in Figure 6a,b. The latter areas occur locally west of Abu Qir Bay, Burullus, Gamasa, the Damietta spit, and north of Port Said (Figure 6a). In general, sands on the nearshore zone (shoreface) of the inner shelf zone include accretionary sand bars that are texturally free of fine-grained particles. These correspond to areas of the highest-energy environments as compared to those on deeper parts of the open shelf area.

Age-wise, surficial sediments on the inner shelf are mostly of recent, predominantly terrigenous sands with heavy minerals, often concentrated as pod-shaped deposits along with lithic fragments, plant matter, recent molluscan fauna, and entire shells and their fragments (cf. Summerhayes et al., 1978 [12]) [13]. These tend to be, for the most part, younger than ~3000 yr BP and accumulated during the progradational phase, when the Nile Delta margin migrated northward (Figure 3, see shoreline of phase II), i.e., when the effects of fluvial sediment discharge exceeded those of littoral erosion processes [30]. It is of note that the nearshore zone acts as a link between the northern delta-coastal sector and inner continental shelf sediment dispersal zones. The gently sloping nearshore zone, in particular, is the area where most energy is dissipated by waves overturning and breaking, thereby inducing marked beach to seabed changes. The lower to deeper parts of this zone extend to the so-called closure depth; beyond this depth, wave action decreases and locally ceases to markedly affect the seafloor and its offshore transport sediment patterns [18]. This effect generally occurs at depths >0.5 of the wavelength L_0 (where the subscript denotes deep water). Sands in this dynamic inner shelf zone are swept as a blanket onto and across the gently sloping seabed and are actively driven largely by the coastal and also partly by the easterly flowing Mediterranean gyre, which achieves velocities of up to 100 cm/s over the shallow shelf [37]. The numerous (55) vibro-cores of ~4 m length, drilled on the inner shelf between the coast and up to an 18 m water depth by the Coastal Research Institute (CoRI), indicate that this area is covered by 1-to-4-m-thick ribbon sands.

It should be added that, more locally, the concave-shaped shores within the inner shelf at Abu Qir Bay, the Gamasa embayment, and the Gulf of Tineh act as the sink zones of converging current systems. In practical terms, these become depocenters, i.e., accumulation sites for sediments received mainly from adjacent eroding beaches (cf. Frihy, 2007 [17]). Such concave convergent-current shorelines foster relatively calmer or lower-energy environments relative to those of the seaward-protruding or relatively straight and long, smooth shorelines of the delta's coastal margin. Relatively lower-velocity longshore currents of 12–17 cm/s were measured along the concave coastal sectors, compared to the higher values at seaward-protruding or relatively straight shores (30 to 46 cm/s; Coastal Research Institute). Unlike the smooth, loose sediments covering the delta shelf to the east, the irregular ridge surface (crests and troughs) that floors the seabed off Alexandria blocks, to some extent, the natural mobility of sands over the rocky inner shelf and also along its contiguous coastline (Figure 3; [9]).

These unique seabed features explain why desert sand was lost rapidly following the artificial replenishment of eroded beaches from 1988 to 1990 (cf. Frihy and Dean, 1992 [57]). This loss occurred because nourished sand placed on beaches and dispersed offshore can no longer return back to the coast in order to maintain the natural equilibrium profile, as it does on a smooth sandy slope.

7.3. Mud-Rich Cones, Prodeltaic and Mid-Shelf Deposits

Mud-rich deposits refer here to admixtures of silty clays and clayey silts (grey pattern in Figure 7), with low proportions of sand (<10%). The mud proportion locally increases to >90% seaward of the active Rosetta and Damietta promontories, where deposits of so-called linear mud deposits accumulate (Figure 4b, Figure 5b, and Figure 7). The mean grain size and sorting results of linear mud deposits range within the silt size ($M_z = 5-8 \phi$) and they are poorly sorted ($\sigma_1 = 1.0-1.5 \phi$). The Damietta linear mud is relatively smaller due to the

lower annual discharge load of this branch (~30%) compared to that of the Rosetta (~70%). A total amount of 18–55 billion m³ of water was discharged annually to the Mediterranean before the construction of the High Aswan Dam and the closure of its reservoir, Lake Nasser, which began filling in 1964 [58]. As a result of continued seafloor grading and displacement processes, the active prodelta muds are commonly bordered by relatively coarser grains of poorly sorted sandy silt ($M_z = 4\text{--}7 \phi$; $\sigma_1 = 1.0\text{--}2.0 \phi$; Figure 6a,b). The prodelta mud is characterized by open marine facies that include benthic foraminifera, shell fragments, echinoderms, glauconite, and mica [12,13].

According to the basic formation processes of classic worldwide deltas [59,60], fine-grained sediment (mud and sandy or silty mud) seaward of the linear mud unit here are prodelta deposits formed as a result of the grain sorting of sediment discharged from the ancient and modern Nile distributaries. In this respect, the seaward bottom currents preferentially erode and displace this mud away and leave a lag of coarser grains (sand and silt) in the coast–inner shelf zone, which forms part of the delta-front environment. The prograded prodelta and delta-front units were deposited further seaward in delta lobes, corresponding to phase II in Figure 4. These formed at the mouths of now-abandoned River Nile distributary channels on what is now the submerged inner continental shelf (cf. Summerhayes et al., 1978 [12]).

In marked contrast to the more laterally extensive seafloor sand-rich sedimentary deposits on the delta shelf surfaces are sectors defined by particularly high proportions of mud, ranging from 80 to 100%. These are shown in Figures 5b and 7, with average sediment sizes ranging from M_z of 5 to 8 ϕ . Those that include such fine-grained deposits occur in three sectors of the mid-shelf trending seaward from a depth of ~12 to 75 m northwest of the Rosetta cone and another toward the northeast of the Damietta cone from ~15 to 25 m; the largest such mud-rich area is oriented west to east at depths from ~20 to 60 m, positioned seaward of the Sebennitic and Athribic channels. These fine-grained sediment sectors may perhaps be among centers of the delta shelf where eroded fine-grained materials had been winnowed, from which the now more sand-rich and sandy silt deposits accumulated. Further north of the Nile Delta, the outer shelf is locally floored by sandy silt deposits ($M_z = 4\text{--}6 \phi$; $\sigma_1 = 2.0\text{--}3.5 \phi$), with < 40% of sand (Figure 7). Previous studies have indicated that some fine-grained sediments in proximity to the outer shelf include relict (palimpsest) deposits that comprise older, reworked calcareous materials such as bryozoans with coralline algae, some carbonate mud, and iron-stained quartz grains [12].

7.4. Major Depositional Sand and Sandy Silt Belts

Farther offshore from the coastal zone, three distinct, long, elongate depositional features extending >100 km in length are recognized between the inner and outer shelf of the delta, herein coded Belts 1, 2, and 3. These linear features shed light on dominant recent to present, largely sand dispersal patterns extending toward the east. The seafloor of Belts 1 and 2 comprises sand-sized material (Figure 5a), and sandy silt is present in Belt 3 (Figures 5b and 7). Unlike the mean grain size, the shelf sediments show an overall seaward increase in the standard deviation (σ_1) progressively from the coastline toward the outer shelf break, i.e., recording somewhat poorer sorting in this direction (Figure 6b). The relatively finer sand on the inner shelf ranges from very well sorted to moderately sorted ($\sigma_1 > 0.5\text{--}1.0 \phi$), while some sectors toward the middle and outer shelf record poor to very poorly sorted values ($\sigma_1 \geq 2.0\text{--}4.0 \phi$). This latter distribution may result from the presence of a mixture of some mud and reworked coarse-grained shells and their fragments. To better characterize these depositional features, they are traced in Figures 5 and 6, which can be combined with the inferred directions of sediment transport in Figure 7. The most notable surficial depositional feature on the delta shelf is sand Belt 1 (170 km long and 15–25 km in width). Information on the current flow intensities and directions affecting these three units are shown in Table 2. On a worldwide scale, similar eroded sand bodies termed belts or ridges are documented as highly dynamic depositional units and have

been described in a number of modern shelf settings, such as those reported by Off [61], Kenyon [62], and Kenyon and Belderson [63].

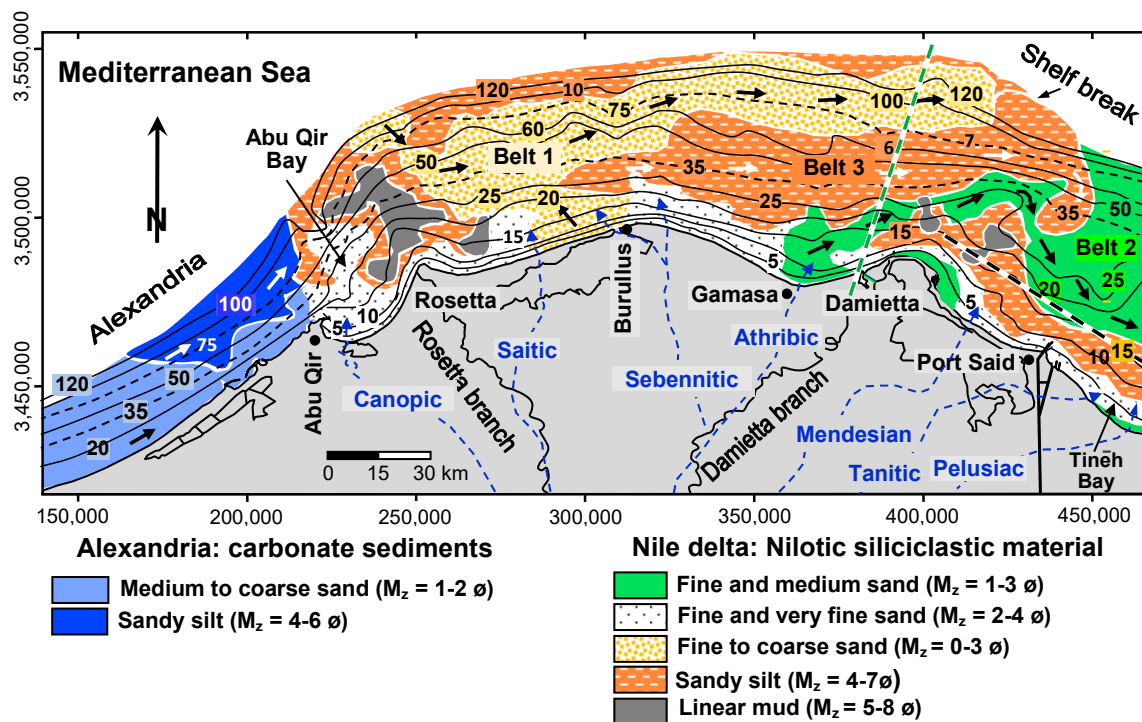


Figure 7. Map of the study area summarizing main characteristics of depositional features of shelf samples interpreted from surficial sediment texture and carbonate content distributions. Also depicted are distinct depositional features (Belts 1 to 3) that indicate directions of major sediment dispersal paths, as shown by arrows. Black dashed line refers to the position of the Manzala fault line [64]; the green dashed line traces the position of the active NNE-SSW Damietta-Lakatka fault zone in this sector (after Stanley et al., 1992 [45]). Map coordinates are in Universal Transverse Mercator (UTM).

7.4.1. Belt 1

Among the most obvious surficial depositional feature beyond the coast on the delta shelf is Belt 1 (yellow pattern in Figure 7), which comprises a sand-sized deposit with a small mud component (<30%). Its mean grain size is fine to coarse to very poorly sorted sands ($M_z = 0.0-3.0 \phi$; $\sigma_1 = 1-3 \phi$), as seen in Figures 5a and 6a,b. It displays an outer shelf to shelf break alignment and extends as a long, relatively straight unit of fairly consistent width, spanning continuously on the upper and middle shelf slope from the northwest of the Saitic headland; from there, it continues arcuately to the east along the eastern Lower Terrace on the remainder of the outer shelf (Figure 7). The southern beginning of this belt covers the upper slope at the Burullus headland, where it consists of relatively coarser and medium sand, and then progressively becomes finer northward along the rest of its arcuate belt. The sediment dispersal pattern of Belt 1 is directed primarily west-to-east by bottom currents, as previously noted by Summerhayes et al. [12].

7.4.2. Belt 2

Further to the southeast, a second, much more irregularly shaped sand body (Belt 2, green pattern in Figure 7) begins from the north of the Gamasa embayment and then extends to the east, covering much of the remaining delta shelf. It accumulated as a more complex-shaped, tighter, arcuate belt on the present gently sloping upper terraces north of Port Said and the Gulf of Tineh basin (Figure 7). It is composed of fine to medium, moderately to poorly sorted sands ($M_z = 1.0-3.0 \phi$; $\sigma_1 = 0.8-1.4 \phi$; Figures 5a and 6a,b).

The eastern part of Belt 2 has been previously reported as extending from the north of Port Said with a tighter turn to the southeast after the Damietta promontory and toward the Gulf of Tineh basin, where it actively moves sediment farther in general easterly to southeasterly directions.

It is of note that the more angular surficial configuration of Belt 2 on the delta's eastern shelf differs considerably from those of Belts 1 and 3, which form longer, narrower, and more gently curvilinear deposits. It is possible that this irregular configuration of Belt 2 may have been a response to a high-speed jet or eddy at >30 cm/s, indicated by Coleman et al. [38] and Murray et al. [52], and/or perhaps one also induced by an underlying seafloor irregularity. The distribution of Belt 2 sediments, primarily its fine to medium sand east of Damietta, bends quite notably landward toward Manzala Lagoon and the coast (Figure 7). It is possible that this distinctive trend may have resulted in part from Belt 2 sediment accumulating on what was a structurally different and possibly more tectonically active sector that had displaced the underlying shelf. This may well have modified the three-dimensional subsurface configuration of the underlying northeastern delta's pre-late Pleistocene to Holocene deposits. In this respect, it is noted that the Holocene sequence beneath the present Manzala Lagoon floor had accumulated in a rhomb-shaped graben basin [65,66] that was likely bound by strike-slip faults. These may be part of the major north-northeast- to south-southwest-trending offset structures that extend toward and into the sector from the northeasternmost Mediterranean and continue southward toward Manzala Lagoon (dashed blue line in Figure 7) and farther into East Africa [67,68]. A green dashed line trending northwest-southeast seaward of Manzala Lagoon (Figure 7) also depicts the position of an active Manzala fault zone structure in this sector, as delineated by Mamoun and Ibrahim [64]. Moreover, the Manzala Lagoon region is underlain by a particularly thick (~3000 m) lower Pliocene to Quaternary section [2]. It is also of note that cores of Holocene deposits taken in Manzala Lagoon record a thickness reaching more than 40 m. This is more than double that of Holocene sequences elsewhere in the northern Nile Delta, where they tend to range, for the most part, from 10 to 20 m in thickness. From these observations, it is possible that some irregular sinuous bends of Belt 2 noted in Figure 7 may represent the effects of the former structural offset underlying the present shelf sediment surfaces and could have diverted this belt north of the present eastern delta coastline.

It appears that the coarse-grained sand in Belts 1 and 2 primarily originated from Holocene transgressive sands. These transgressive sand facies have generally low fine-grained particle content and some comprise iron-stained relict grains [31]. As the sea level rose from 12,000 to 8000 yr BP, the high-energy shoreline migrated landward (southward), which led to the reworking of the former subaerial plain deposits, up to 30 km south of the present delta coastline, thus forming littoral and nearshore marine transgressive sands, coded as Phase I in Figure 4. Sediments of these transgressive sands were subsequently reworked and laterally dispersed in shore-parallel, curvilinear, coarse-grained sand Belts 1 and 2 over time by seabed Holocene to modern shelf currents. These two units help to position the former coastal to inner shelf environments of Holocene sea level stands. Such an interpretation will be further supported in the forthcoming section that discusses the distribution of land-derived heavy minerals in shelf sediment deposits.

7.4.3. Belt 3

In contrast to Belts 1 and 2, the broad, finer-grained sandy silt Belt 3 (orange pattern in Figure 7) is identified in the inner and middle shelf of the delta (Figure 5b). This belt (150 km long and 8 to 27 km wide) is composed of a poorly sorted sandy silt sediment ($M_z = 4-7 \phi$; $\sigma_1 = 1-2 \phi$). It has lower sand content, reaching less than 15% (Figure 6a,b). In view of its sediment transport trend, the dispersal pattern of this belt also shows some similarity to that of the straighter, narrower, and more distinctly coast-parallel Belt 1, as it is also, for the most part, directed primarily from west to east (Figure 7).

The configuration and sediment characteristics of the broad, fine-grained sandy silt forming Belt 3 suggest that it is most likely related to processes of transport and deposition off the Burullus central plain via the Nile's relict Sebennitic branch. It likely was once

positioned across the subaerially exposed continental shelf during the last Holocene low-sea-level stands (Figure 4, Phase II). Inasmuch as it lacks prodelta and delta-front deposits from off the Sebennitic branch, this belt (Figure 7) is proposed to have been formed in response to the continued action of grain-sorting processes, dispersion, and the displacement of the Holocene progradational delta plain of Sebennitic branch sediment by the wind- and wave-driven east-trending bottom currents. These deposits may also have been displaced in part by the Eastern Mediterranean counter-current gyre. The large amount of original delta plain sediments forming this branch was dominated by sandy and mud-rich deposits, which incorporated channel fill, marsh, and lagoonal facies, totaling a 10 to 20 m thickness. Such deltaic deposits began to accumulate at approximately the time when the rate of sea level rise began to decelerate, from roughly 7500 yr BP to the late Holocene [31]. The mouth of the Sebennitic was once located further north, on what is now the inner to middle delta shelf [29,66].

8. Carbonate Displacement

As discussed earlier, the primary source of carbonate sediments covering the beach and seabed off the Alexandria sector (light and dark purple pattern in Figure 7) originates from the erosion of the linear coast-parallel limestone ridges of Pleistocene age, shown in the lower map of Figure 1 (cf. Shukri et al., 1956 [3,4]). The area of markedly higher proportions of carbonates in the westernmost part of the Alexandria shelf (>80%) progressively decreases to 40–60% toward the east, north of Abu Qir Bay, where they merge and are masked by siliciclastic sediment input of Nilotic origin. This supports evidence of a prevailing NE dispersal trend, i.e., nearly parallel with the coastline (Figure 8). This transport pattern also suggests a mean grain size fining trend from the west (coarse to medium sand) toward the east (sandy silt) at the Abu Qir Peninsula (Figure 5a). Such textural and compositional trends are interpreted as markers of the net northeasterly driven currents that prevailed from along the Alexandria margin and then further laterally to the northeast, where they merged with the Nile's siliciclastic materials (Figure 7, see arrows).

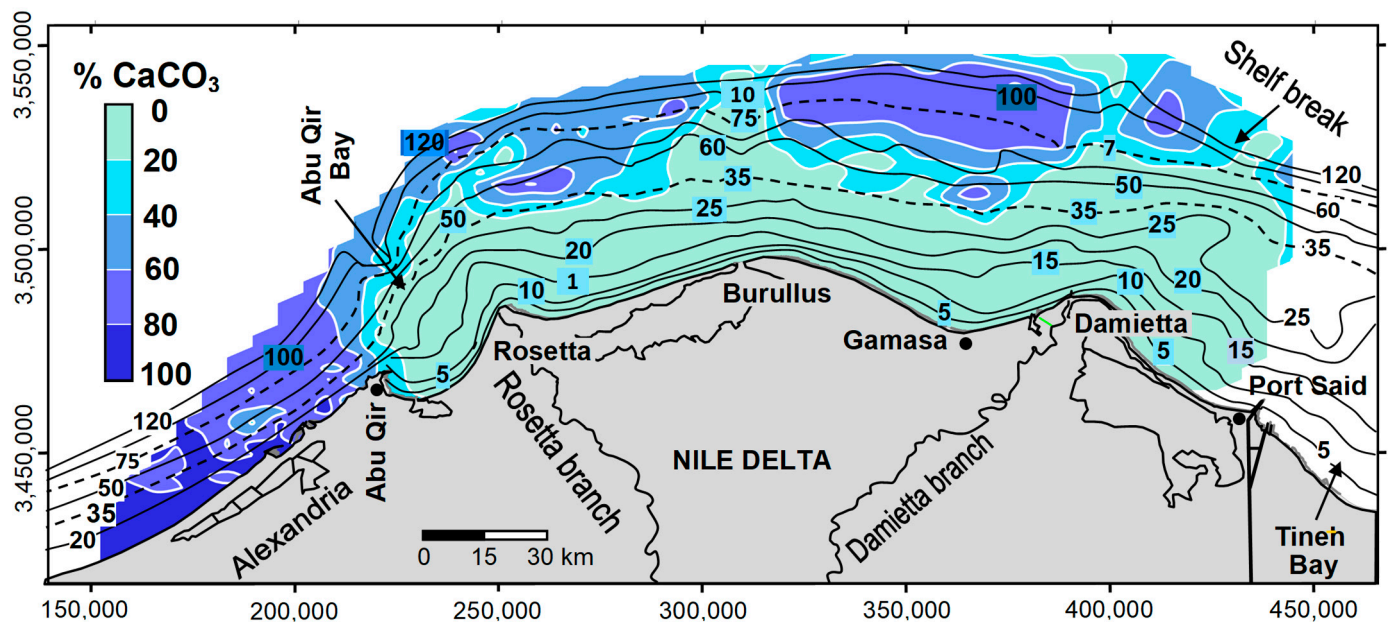


Figure 8. Spatial distribution of proportions of carbonate content in selected sediment of the study area. Relatively higher values of carbonate content occur across much of the Alexandria shelf sector and on some lower terraces and the outer shelf of the delta farther to the east. Map coordinates are in Universal Transverse Mercator (UTM).

Farther east along the offshore margin of the Nile Delta, a marked pattern of a moderate proportion of carbonates (40–60%) prevails as a broad coast-parallel zone on the middle and outer shelf (>70 m water depth), shown in Figure 8. Sediments of this zone are dominated by a mixture of carbonate mud, reworked infralittoral faunal shells and fragments, and relict (palimpsest) iron-stained sand grains [12,14]. The moderate proportions of carbonates in this zone progressively decrease to the south (<20%) across the inner shelf toward the coastline. Such a shoreward decreasing trend indicates that the carbonate content in this zone, at best, acts only as a partial carbonate feeder source to the inner shelf. This should by no means be interpreted as a function of overall long-distance, offshore-to-land-directed carbonate transport dispersal, since recent molluscan shells and those of other carbonate-shelled organisms living on the inner shelf zone of the delta also serve as a carbonate source.

It is noted that in shallower and gently sloping areas, there has been a cross-shore component of sediment movement, with the erosion of beach faces and inner surf zones and the seaward-directed transport of the eroded sand toward offshore and longshore directions. This is inferred from the analysis of the sorting patterns of heavy minerals in a series of sediment samples collected along cross-shore profiles that extended to approximately a 6 m water depth at a distance of ~1000 m from the coastline [17].

9. Heavy Mineral Concentrations

The widespread geographic distributions of heavy mineral concentrations in the examined samples range from <1% to 14% (Figure 9). Of special interest are the pronounced higher concentrations of heavy minerals (>6% to 14%) that extend locally as isolated lobes from the present shoreline onto the open seafloor for a maximum of ~15 km (in light blue and purple pattern in Figure 9). The extreme concentrations found in these lobes decrease rapidly in the along- and cross-shore directions. It is of note that most of these pronounced mineralogical features occur closely to the position of the Nile Delta's seaward extension of its former, now-extinct branches that flowed to the coast during progradational evolutionary Phase II of the delta (see Figures 4c and 9). This suggests that these distinct features are related to remnant distributary mouths and estuaries of these former Nile branches. These now-extinct and sediment-filled north-trending distributary channels occur laterally south of the present coastline, from slightly east of Alexandria to Abu Qir Bay, and then all the way to the east of the Suez Canal in the Sinai Peninsula, hundreds of kilometers to the east, as shown in Figure 9.

These mineral features appear to coincide geographically or are close to the Holocene lobes of the delta-front and prodelta of the River Nile distributaries now buried in the northern delta's coastal plain, as interpreted from petrologic analyses of numerous long cores drilled south of the coastline [30,40]. These depositional lobes originally formed at the mouths of former Nile distributaries flowing to the Mediterranean (Figure 2). After the accumulation of these lobes during the progradational evolutionary Phase II period of the Nile Delta in the early to late Holocene (Figure 4), they were eroded and reworked by prevailing east-trending longshore and bottom currents. This led to their formation as distinct concentrations of heavy mineral deposits displaced primarily eastward and offshore.

It has been noted that the location and orientation of the identified lobes offshore do not in all cases coincide with most of the inland traces of former deltaic branches such as the Saitic, Sebennitic, Athribic, and Mendesian (Figure 9). This relative offset could be related to the continued lateral shifts of their estuaries mostly to the east, and some locally to the west [29]. This may have been caused by the effects of periodical reversals of wave-induced longshore currents or by other physical interventions on the seafloor, as shown in Figure 3. The laterally wider extension of markedly higher heavy mineral concentrations (8–14%) on both sides of the presently still-active Rosetta promontory, and to the east of the Damietta branch and also off the ancient Sebennitic estuary, also confirm their natural displacement along the delta coastline (Figure 9). An example of this shift has been recorded for the Sebennitic channel that formed the remnant Sebennitic promontory,

now the largely eroded and rounded Burullus bulge of the north–central delta [29,31]. The mouth of this branch (one extending to a depth of 18 m) shifted three times toward the west as a result of the progressive overall lowering of land relative to the sea level in this northern region, estimated at a rate of 7.7 mm per year [69].

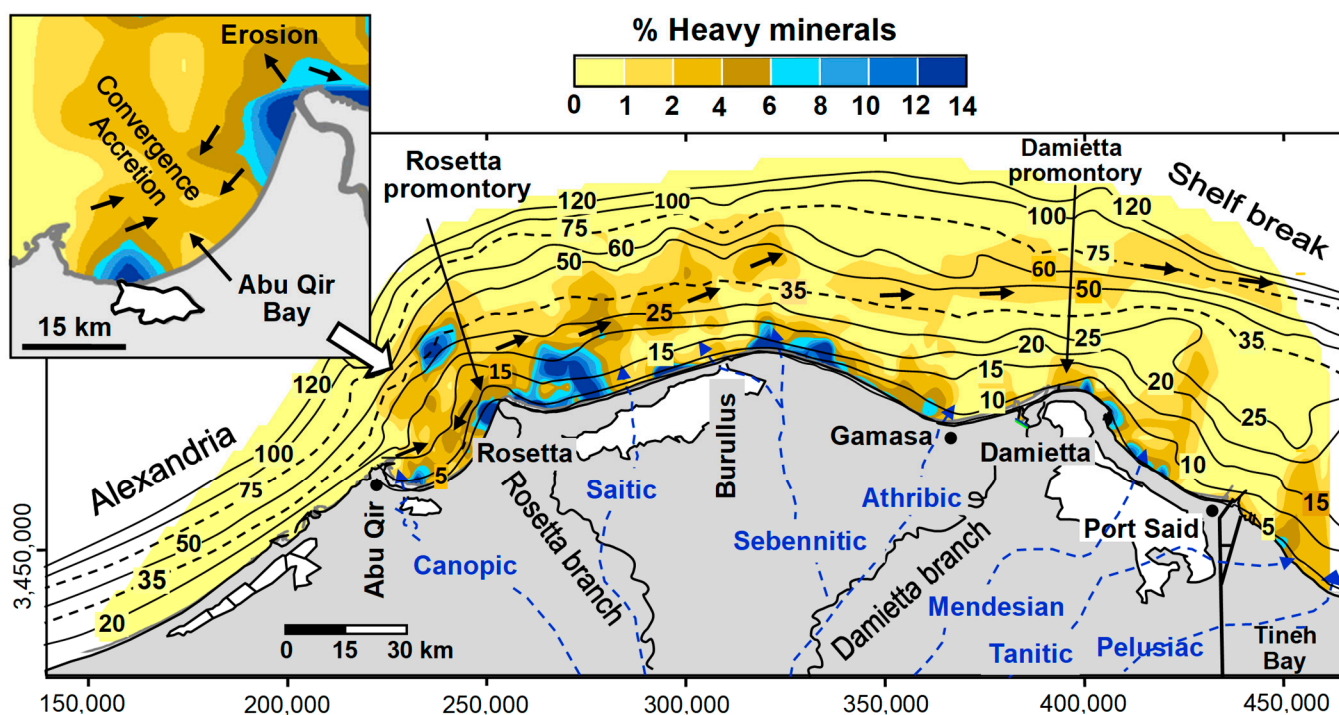


Figure 9. Spatial distribution of heavy mineral proportions in surficial beach and shelf samples of the study area. Relatively higher values of heavy mineral concentration (to ~14%) generally denote remnant estuary lobes of former Nile distributary channels that formed during the seaward progradation Phase II of delta evolution (in Figure 4c). Heavy minerals at these relict estuaries have been intensively concentrated from continued erosion and reworking of original estuaries during return landward regression of Phase III that resulted in the present arcuate delta shore. Inset map enlarges the dispersion pattern of heavy minerals in Abu Qir Bay, indicating low (convergence) and high (divergence) energy levels. Direction of prevailing sediment transport is indicated by arrows. Map coordinates are in Universal Transverse Mercator (UTM).

A higher percentage of heavy minerals (8–14%) is found in the along-shore and inner shelf of the remnant Burullus promontory. Further inland of these relatively rich heavy mineral centers lies the coastal dune belt (~16 km long by 0.3–1.0 km wide, and up to 20 m elevation) that formed from the extensive erosion of the relict Sebennitic promontory (~30,000–3000 yr BP), which was located further seaward and to the north on what is now the inner to middle shelf [66]. The continued shoreface and coastal plain erosional processes tend to selectively remove less dense quartz and feldspars and sort and concentrate the heavy minerals, or ‘black sand’ placers, as dense concentrated lag deposits in the active dune belt formed on the central Burullus coast. This dune belt is now being mined by the Egyptian Black Sand Company. It is estimated that the net commercial/economic heavy mineral reserve is roughly 238.5 million tons, with an average concentration of 3.39%, which is sufficient to keep the company operating for approximately 16 more years [70].

Similar to the dynamic processes that now operate at the beaches of the presently active delta promontories (see pattern of arrows in Figure 3), the pronounced seaward extension of estuary lobes during Phase II (Figure 4c) has resulted in erosional processes of wave convergence associated with longshore current divergence. These processes have caused the intense local erosion of these delta lobes, which, in turn, tend to selectively

remove less dense minerals, such as quartz and feldspars, and concentrate heavy minerals as a lag deposit. It is expected that the original coast formed by such lobes will be, in time, increasingly smoothed into an arcuate shape. Presently, similar hydraulic sorting processes are noticed on other recent deltas, in which heavy minerals or placers are highly concentrated on opposite shores of the modern river mouths, where physical processes could have potentially concentrated these denser minerals. Examples occur at the Rosetta and Damietta Nile delta promontories [17], and comparable ones have been noted at the fluvial mouths of other deltas elsewhere, such as that of the Columbia River [71,72].

A similar grain-sorting transport process presently occurs in front of the Rosetta promontory, creating divergent longshore sediment dispersion where sand moves to both the east and west away from the mouth [17]. Thus, one can envision the original morphologies of relict estuaries being significantly modified as they prograded seaward during their formation in the early to mid-Holocene. Following this phase, they subsequently retreated landward from their former positions at the inner shelf (10–15 m water depth) in the late Holocene to one at the present coastline. This landward shoreline retreat, corresponding to Phase III, was defined by Stanley and Clemente [41] and is shown in Figure 4. Hence, we interpret the considerable local concentrations of heavy minerals observed along the Nile shelf as markers of ancient Nile estuaries at or near the mouths of the former delta's fluvial branches. This phenomenon has also been noted in the modern marine settings of continental margins elsewhere [71–73].

The heavy mineral lobes of the Athribic branch in the Gamasa embayment and of the Pelusiac branch in the Gulf of Tineh east of Port Said (Figure 9) did not develop well because of the local shoreline geometry at these localities. Their estuaries were positioned on a concave-shaped coastline that faces seaward and which is a zone of current convergence flow. This resulted in sand accretion and can be considered a depositional sink, similar to the schematic depicted in the inset showing Abu Qir Bay (Figures 3 and 9). This morphodynamic mechanism appears to have silted up their estuaries as a result of prograding accreted beach sand and coastal bar formation. Until recently, a series of accretionary shore-parallel shelly coarse sand was observed on a wide delta plain surface south of the Tineh Gulf to the east of Port Said [74]. The shoreline fronting these prominent ridges reveals a progressive advance of 12 m/yr [75]. Along this coastal stretch, the percentages of heavy minerals decrease eastward as a response to longshore transport. Here, beach sand is progressively diluted by the light grain components formed by relatively high concentrations of shell fragments and coarse grains of quartz, thereby masking otherwise heavy mineral accumulations. This process eventually led to the closure and burial of the relict Pelusiac channel.

A similar accretionary mechanism has diluted the concentration of heavy minerals along the embayment at Gamasa (Figure 2). The shoreline of this concave-shaped sector facing seaward is presently accreting at an average rate of 4.2 m/yr [17]. Further offshore of the delta shelf, considerably moderate values (<6%) of heavy minerals are spread more evenly on most of the middle shelf, followed by a progressive decrease (<1%) toward the outer shelf break. As the continental shelf of Alexandria is influenced in large part by its carbonate-rich province, much lower heavy mineral content (<1%) also occurs on the seafloor of this sector (Figure 9). Nevertheless, somewhat higher concentrations of heavy minerals (1–4%) are distributed in the curvilinear belt that is distinctly coast- and contour-parallel. This belt extends from the Rosetta promontory to the east of Damietta on the middle shelf between 35 and 60 m water depth (Figure 9), suggesting the influence of bottom currents sweeping extensively to the east (Figure 7, see arrows). The position of this belt likely marks the former coastal to inner shelf environments by altered sea level stands that evolved during the late Pleistocene to the Holocene. As the sea level continued to rise, heavy minerals in the original belt were sorted and concentrated on the seafloor by Holocene to modern shelf currents. Through time, however, the concentrations of heavy minerals in this belt have been progressively depleted due to the effects of continued sorting and reworking by transport processes.

Heavy minerals in Abu Qir Bay serve as a good example to identify localities along the coast where there are changes in energy levels, usually associated with either increased erosion or deposition. The high concentrations (8–14%) of heavy minerals there are due to the effects of erosion, and these also help to interpret the effects of flow divergence in a direction away from the high-energy area near the tip of the Rosetta promontory (Figure 9, enlarged Abu Qir Bay map). An area of lower concentration of heavy minerals (<2%) is noted in a region to the west, where flow convergence results from opposing bottom currents that meet toward the center of this bay, i.e., current convergence (cf. Frihy et al. 1994 [76]), which is interpreted as a sediment depositional sink. This interpretation is confirmed by studies of wave refraction and sediment transport patterns along the Nile Delta coast (Figure 3).

In addition to studies of wave refraction and sediment transport patterns along the Nile Delta coast, this interpretation is also confirmed by the slow-velocity bottom currents measured separately twice in the center of Abu Qir Bay [36,50]. The majority of the currents (93% of the time) measured by these authors were less than 6 cm/s. The slow current velocity in this particular area may be responsible for the formation of accreted beach sand and coastal bars, which, in turn, led to the silting of the mouth of the former Canopic branch. Likewise, this mechanism emerged at the Pelusiac distributary channel east of Port Said. These observations are clearly visible in the field, where a large number of whole shells and fragments together with floating mica flakes accumulate on the beaches of these particular low-energy coasts. In practice, coastal projects implemented in such areas (lagoon inlets, harbor entrances, and power plant water intakes) are experiencing sedimentation hazards that require regular bottom dredging to maintain safe and appropriate depths.

10. Long-Term Sediment Dispersal through Time and Space

Unlike the dynamic forces that directly influence the coastal–nearshore sediments, those acting on the deeper parts of the delta shelf have received little attention. However, Inman et al. (1992) [37] disclosed that the inner shelf sands of the Nile Delta appear to be primarily driven by the easterly flowing Mediterranean counter-current gyre that achieves velocities of up to 100 cm/s. This transport process is undoubtedly enhanced by wave action, primarily during winter storms. In post-storm events, the accumulation of numerous beach pebbles together with patches of coarse clean sands with shells that are observed on the delta's beaches have served as evidence to indicate off-to-onshore sediment transport paths [77,78]. They indicate that such beach pebbles originated from the seabed erosion of remnant consolidated mud and the sandstone alluvial banks of the former Nile branches, which are now buried in the upper traces of the shelf (see positions of these banks, Figure 2). The coarse-grained sands (average medium diameter of ~1.0 ϕ or 0.5 mm) were derived from the erosion of relict offshore sand sources, identified here as Belts 1 and 2. Storm waves may have driven parts of such sediments from their offshore sources toward the coast.

The offshore shelf variations of significant wave heights, from 1975 to 2015, derived from the DHI's Mediterranean Wind Wave Model (MWWM), indicate the periodic occurrence of storm wave events at two stations offshore of the Nile delta [79]. Waves were calculated at water depths between ~20 and 30 m over 40 years and extracted at 1-h intervals. The time series wave variation revealed that the strongest storm events of >6 m height occurred approximately once a year, in winter (during December–February). The results of the study indicate that storm events affecting the deeper zones of the Nile Delta shelf (middle and outer shelf areas) may have to be considered to be as dynamically active as those in nearshore areas. As a result, post-storm bottom currents might affect the shelf seafloor more than once per year, causing turbulent eddies that, at the least, are capable of modifying and adding to bottom currents on the open shelf. During a winter storm, a high-velocity bottom current of 113 cm/s was recorded at a water station depth of 125 m above the upper slope, one that lies above a seafloor depth of ~400 m and seaward of the shelf-break [51].

Progressive sorting from diverse dispersal processes affects grain sizes, which vary from sand to mud, and the concentration of heavy minerals, and their separation from a mass of less dense grains can help to interpret sediment transport mechanisms. These respond to the variety of energy levels and dispersal conditions that can prevail in the different study areas. In general, the important and distinct accumulation of specific mineral sizes and densities at the coast and on the inner to outer shelf sectors helps to determine how such specific areas have been influenced by various, and sometimes distinct, transport energy levels and thus provide information on their depositional origins. However, in most cases in the study area, we are unable to specify the timing or the energy intensity indicators at localities that could have been provided by the depth of closure by using heavy mineral density data (Figure 10a). Moreover, in strong but variable bottom current environments, the dating of a sand–mud line formation, as provided by measurements of mineral size boundaries that show a complete transition from sand to silty mud to mud-rich deposits on the seafloor, are difficult to define (Figure 10b). These challenges are, in large part, a result of the timing of the component, i.e., where there have been long periods of mixing and then additional remixing of sediments on the seafloor that were affected by transport currents of variable intensity and direction over the years, which affected different shelf surfaces at various times. In the present study, we are in effect evaluating the former displacement events through time as well as recording the modern to ongoing mixing of these previously reworked (palimpsest) and recently moved deposits.

On this continental shelf, one usually encounters the partial preservation of earlier depositional effects that are masked in some manner by the influence of subsequent to present dispersal patterns and mechanisms. Thus, the attributes of grain sizes presently measured, plus the diminution or increased relative abundance of certain surficial minerals of various sizes and densities now present, were likely formed earlier on the delta and shelf by previous transport intensities and depositional events. Thus, examples of material now collected at the Nile Delta's shelf surface can include reworked, older, relict, stained siliciclastic mineral grains and/or eroded and now-displaced shallow water marine shells recently collected in surficial deeper water sediments at unexpected living depths.

For example, one finds on the shelf an absence of progressively increasing silt and clay-sized material (mud-rich zones) at what appear to be the more distal surfaces of the large sand-rich belts toward the eastern end of the present Nile Delta shelf (Figure 7). Thus, there are few clear examples of firm evidence for sand-to-silt-to-mud transitional marker zones at present depths at the eastern delta. However, it is recognized that the sea level was considerably shallower in the past, during the early to mid-Holocene. Exceptions to this may be the two linear mud belts at mid-shelf depths depicted in uniform grey patterns (Figure 7), one on the mid-shelf trending NW ~40 km seaward off the Rosetta cone and the other trending NE ~20 km seaward of the Damietta cone (Figure 7). These appear associated with the two youngest and still-active major existing Nile distributaries, whose sediments, in the past, and perhaps until recently, may have reached and extended well beyond the coast via cross-shelf processes. We also note the larger mud-rich belt that trends west to east, north of the Sebennitic to the Athribic, that may also be a recent deposit formed as related to, or influenced by, Belt 3. The mass of eroded mud material elsewhere on the shelf appears to have accumulated as far seaward as the continental slope at depths of 200 m or more as the vague mud line in Figure 10b, well below the shelf break. Once released at these depths, they can move further downslope via periodic gravitative current flows onto the Nile cone and even deeper onto the eastern Mediterranean Levantine basin floor [80,81].

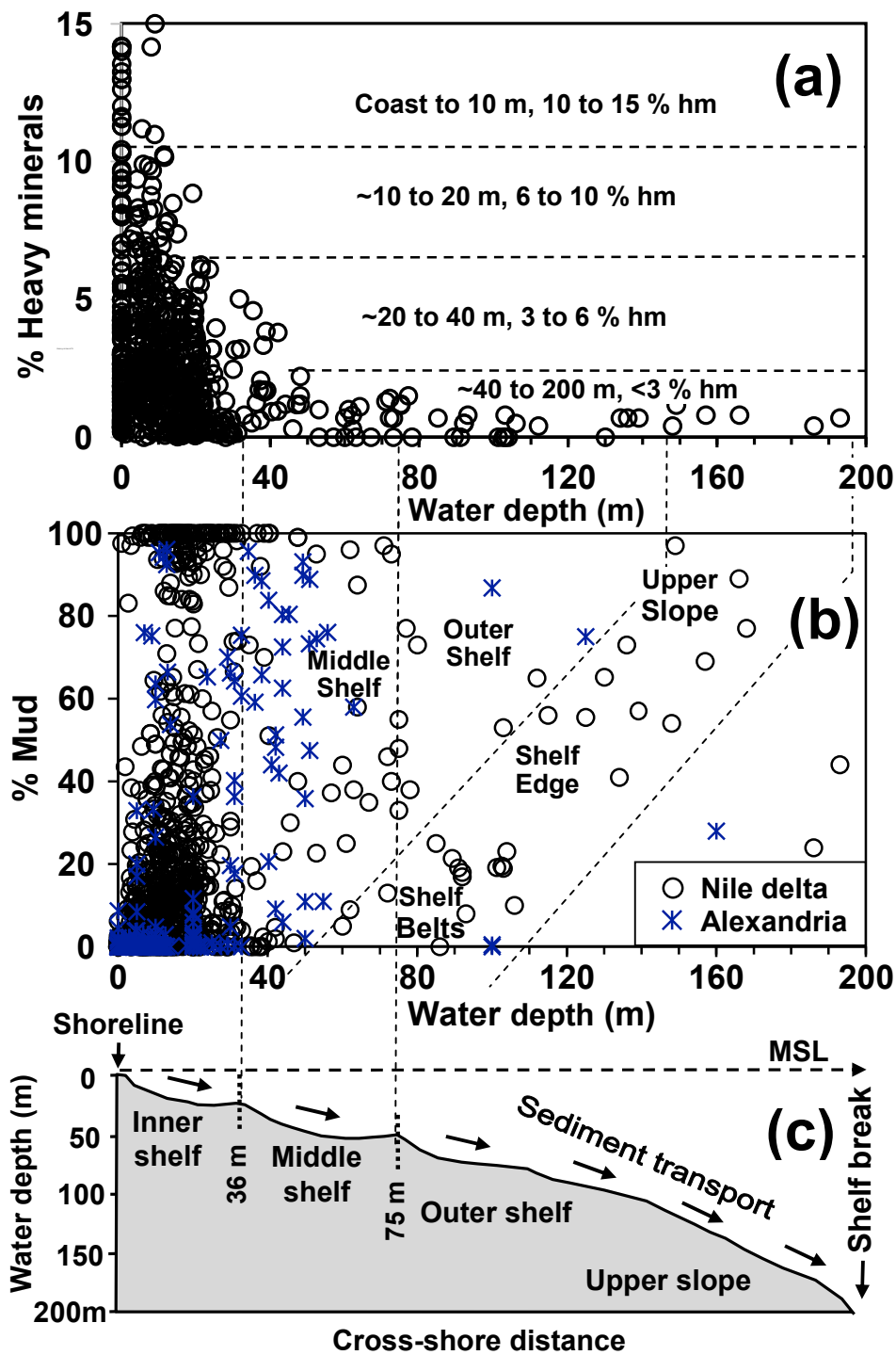


Figure 10. Bivariate plots of water depth in meters versus relative percentage of heavy mineral (hm) concentration (a) and percentage of mud (b) in examined samples. Both plots compiled to seek information on depth of closure and sand–mud line, both defined in text, which are difficult to distinguish clearly due to various mixed dispersal patterns and extent of reworking on different parts of the delta shelf. (a) reveals some associations between heavy mineral percentages and depth; (b), on the other hand, does not clearly distinguish between percentage mud and depth (see discussion in text). (c) Generalized cross-shelf seabed topography depicting offshore trending bottom and downslope gravity currents (arrows) responsible for displacement of light and heavy minerals to deeper water, some beyond the outer shelf edge.

The other marker of sediment transport effects cited above uses dense heavy minerals vs. less dense siliciclastic sediment, such as quartz and feldspar grains, to show displacement by Nile distributaries and bottom currents onto the coastal marine sectors and locally as far as the mid-shelf. Plots showing where pods formed largely of heavy mineral concentrates presently occur along and northward of the shelf's coastline appear in the maps in Figures 4 and 9. A plot of heavy mineral concentrations vs. water depth is shown in Figure 10a and indicates that concentrations of less than 3% occur at a depth of the inner to mid-shelf of around 40 m. This 'break' is somewhat more distinct than what is shown by the percent mud vs. depth, which records a much less clear preferential depth zone, at a very approximate ~80 m on the open mid-shelf (Figure 10b). The latter indicates that small particles of silt and clay, of considerably lower density than heavy minerals, can be moved much farther and deeper by bottom currents active at the shelf's seafloor surface, and they can be displaced across more variable depths.

Focusing on the Nile Delta's offshore shelf sector, a depth of closure of 20–24 m on the open shelf proper has been determined from the systematic analysis of historical bathymetric maps surveyed in 1920, 1976, and 1984 [35]. These values exceed slightly the slope breaks on the shelf, which occur at 14 to 18 m water depth [11]. In comparison, and due to the steep slope off Alexandria, the position of the offshore boundary separating the recent and relict stained sand facies has been used to define a depth of closure there at between 8 and 10 m.

11. Conclusions

Mapping the proportions of sand and mud, the mean grain size, the standard deviation (sorting), heavy mineral concentrations, and carbonate content along the coast and in the bottom sediments of the various Alexandria–Nile Delta shelf sectors provides useful information in this study. These aspects help to interpret the classical evolutionary phases of the Nile Delta from the late Pleistocene to the present. Two distinct sediment sources have contributed to the study area: those of Nilotic fluvial siliciclastic and those of carbonate-rich origin. Sands off the Alexandria beach and shelf are derived in large part from the erosion of the Pleistocene shore-parallel limestone ridges that partially cover the nearshore and backshore environments that comprise biogenic and carbonate-rich sands, whereas, east of Alexandria to the Abu Qir headland, sediments are more directly influenced by the River Nile's fluvial siliciclastic input.

The reworking and dispersal of the Nile flood sediments from several former and two modern distributary channels have resulted in major conspicuous depositional features that floor the inner and middle shelf areas. These include the prodelta muds that are associated with the present-day delta's Rosetta and Damietta promontories, and the three coast-parallel linear to curvilinear belts that are related to the three major coarser depositional phases of the delta's evolution. Among these belts, two comprise very fine to coarse-grained sand (Belts 1 and 2) and the third (Belt 3) is formed of sandy silt (Figure 7). The geometric configurations of these features serve as dynamic indicators to infer the present dominant unidirectional currents sweeping the seafloor in an easterly and not a coast-to-seaward trend. Such currents were driven by dominant active currents during most of the Holocene that resulted from the prevailing NW winds and waves, in conjunction with the dominant offshore counter-clockwise gyre of the Eastern Mediterranean flow. It is suggested that Belts 1 and 2 originated from processes of erosion, reworking, and lateral dispersion of former early Holocene marine transgressive sands by dominant seabed shelf currents. These two belts, in turn, may help to position the former coastal to inner shelf environments during some previous Holocene sea level stands.

Mapping the proportions of heavy minerals helps to identify the former positions of the Nile Delta's extinct estuaries that flowed to the coast during the prograding evolutionary Phase II period of the delta in the early to late Holocene (Figure 4). Earlier coastal phases were similar to what is now taking place at the two modern Nile River mouths. They likely were followed by the intense erosion of the original deltaic channel and estuary

lobes, which, in turn, resulted there in the formation of heavy minerals concentrated as lag deposits.

As noted, it is difficult to clearly identify the depth of closure and especially the sand–mud line, as is considered herein (Figure 10). This likely results from an attempt to evaluate the entire present superposed database from all shelf environments together and their considerable original variability, as well as continuous mixing by bottom currents of relict to modern depositional patterns of shelf depocenters through time. This would have mixed earlier deposits from now-buried ancient seafloor sequences with more recent materials from younger branches of the Nile. Not surprisingly, the sediment patterns of earlier depocenters would have been considerably dispersed by multiple successive dynamic processes that likely altered the original textural and mineralogical attributes. The mixing of the various amounts of mud to sand and heavy mineral concentrations at water depths from different environments could at best be identified by a detailed study of dated sediment cores and shallow high-resolution seismic profiles collected across the shelf. Such materials could help to determine the original timing, depth, and locality at which these earlier wave energy parameters occurred.

From a practical point of view, the results of this study indicate that the search for marine ‘black sand’ heavy mineral placers will need to focus preferentially on the inner shelf areas that incorporate buried traces of relict estuarine lobes of now-buried ancient fluvial branches. Additionally, the generated maps highlighting detailed sediment attributes and evolving coastal configurations as defined here could also be used by Egypt to assist in developing future engineering protection projects. With Egypt’s increasingly vulnerable coastline, it would be helpful to implement more effective coastal protective structures and climate change adaptive measures, with safer urban near-shore development and the appropriate positioning of additional gas and oil extraction facilities. In this respect, it may also be suggested that channel maintenance dredged sediments derived to alleviate problems in navigation channels, river estuaries, coastal lagoon inlets, and power plant water intakes could rather be recycled for the separation of their heavy minerals, instead of releasing them offshore as waste material.

Sediment yields from the present River Nile into the Mediterranean have almost ceased as a result of the construction and closure of the Lower and High Aswan dams and entrapment in their reservoirs in Upper Egypt. Moreover, the diminished amount of Blue Nile water, reduced as of 2022 by the closure of the massive GERD Dam in Ethiopia, coupled with the continued high evaporation rates affecting Lake Nasser Reservoir water positioned in the Eastern Sahara, together, will inevitably affect sedimentation patterns in Egypt, the Nile Delta, and its adjoining coastal and offshore shelf sectors. In the absence of sediments from the river, wave-induced currents combined with the Eastern Mediterranean gyre are actively inducing a seriously diminished disequilibrium, not only on the coast but also of sediments now available for the overall coastal and shelf budget. In the long term, and as the deeper sectors of shelf sediments become dynamically active, they will change from the present-day quasi-balance to one out of balance, and perhaps to one recording a negative sediment budget. It is expected that the continued depletion of the nearshore zone sand budget will, over ever shorter times, accelerate processes of wave-induced erosion. In addition, Egypt’s vulnerability at its populated low-lying northern delta margin is increasing substantially as the sea level continues to rise and the shelf substrate is subsiding [82]. This is by no means a newly developed situation, as indicated by archaeological evidence of a Greek city dating back to ~750 BC in the western Abu Qir Bay [83,84], which, at approximately 700 AD, became submerged below sea level, and presently lies at a depth of –6 to –7 m completely beneath the water surface.

The present study of geologically recent to ongoing surficial sediment distribution and dispersal across much of the Nile Delta shelf provides an extensive database, one updated herein to more closely focus on where and how recent sediments have extended from the coast to the outer shelf break from the Holocene to the present time. This examination is promoted in view of two serious problems now affecting Egypt. These are the extensive

coastal erosion due in part to the sea level rise and the subsidence of the seafloor and northern delta margin, and the influence of decreased fresh fluvial water while saline water now enters landward to as far as the mid-central delta. This latter is amply recorded by the pumping to the surface of saline groundwater over a large area of the delta. The amount of freshwater readily available to Egyptians is now among the lowest per inhabitant in the world. Thus, more information is required to help implement and position effective safeguards at present to ensure, to the greatest extent possible, that less salt water intrudes onto land and under land surfaces into the delta's essential fresh groundwater supplies. The decrease in the Nile's freshwater now lowers Egypt's much-needed agricultural production, amid rapidly growing essential population and industrial needs. The direct connections between the much-reduced Nile freshwater supplied on land and the increased role of saline offshore realms on the delta itself now need serious consideration and planning. Among those offshore attributes that appear to warrant serious focus are those that may help to delineate and reduce the subbottom pathways of salt water from the offshore shelf to land. For this, a combination of three-dimensional offshore measurements is now required, in addition to the data on surficial sediment distributions presented in this study. Efforts needed include recovering an extensive database on the shelf using moderate depth drilling that reaches the Pleistocene substrate for the recovery of datable core sections, and also a closely spaced network of high-resolution subbottom seismic profiles. This additional detailed geological and geophysical information, along with the network of surficial sediment data herein, will allow closer correlations to be made between the offshore and deltaic land sectors than those now available. These proposed integrated studies could assist coastal engineers in developing practical protection applications. They may, at a minimum, further detail the rates of stratal subsidence and substrate offset, which now need to be more closely identified and measured between the offshore and the low-lying delta proper. The expected increase in the rate of sea level rise, and also in temperatures and aridification on land during this century, combined with minimal Nile freshwater and sediment input, along with Egypt's continued population growth, now require intensifying, multi-disciplinary research in this study area. This effort has now become much more than a provincial and purely theoretical academic exercise.

Author Contributions: O.E.F. focused on the attributes of the Nile Delta coast and primarily offshore sediment dynamics on the different delta shelf sectors; J.-D.S. integrated geological and stratigraphic research results applicable to the adjacent subaerial Nile Delta area, and some sectors locally seaward on shelf, and beyond to deeper water settings on the slope to the southern Levantine Basin. All authors have read and agreed to the published version of the manuscript.

Funding: This research received no external funding.

Acknowledgments: A major part of the samples examined herein were collected by the STDF-528 project (Science and Technology Development Fund) financed by both the Academy of Scientific Research and Technology and the Coastal Research Institute (CoRI) in Egypt. The first author of this article was the PI of that project. Our appreciation is also expressed to the Woods Hole Oceanographic Institution for generously providing samples from R/V Chain Cruise 119 used herein. We thank colleagues and technicians who participated in the field and laboratory activities of this study. O.E.F. expresses his appreciation to colleagues Essam Deabas and Mohamed Hassan for their help in data processing, and Mohamed Said and Ebtessam El Sayed for providing the data on currents. The second author acknowledges the assistance for many years of the international team of researchers with the Mediterranean Basin (MEDIBA) Program, who participated with him in the field in Egypt's Nile Delta, and the laboratory at the MNH-Smithsonian Institution, Washington D.C., for the Nile Delta study program from 1983 to 2016. Funding for previous program studies were generously provided to J.-D.S. for many years by the Smithsonian Institution, but none were provided since his retirement eight years ago. Sarah E. Wedl helped the authors to prepare the manuscript for publication. J. Dronkers and M. K. El Sayed provided insightful suggestions for the authors. We would also like to thank three anonymous reviewers for providing valuable comments and suggestions that also helped to improve the manuscript.

Conflicts of Interest: The authors declare no conflict of interest.

References

1. Ball, J. *Egypt in the Classical Geographers*; Government Press: Cairo, Egypt, 1942; p. 203.
2. Said, R. *The Geological Evolution of the River Nile*; Springer: New York, NY, USA, 1981; p. 151.
3. Shukri, N.M.; Philip, G.; Said, R. The geology of the Mediterranean coast between Rosetta and Bardia. Part II. Pleistocene sediments: Geomorphology and Microfacies. *Bull. Inst. Egypt* **1956**, *37*, 395–427.
4. Butzer, K.W. On the Pleistocene shorelines of Arabs' Gulf, Egypt. *J. Geol.* **1960**, *68*, 626–637. [[CrossRef](#)]
5. Zaid, S.M.; Mamoun, M.M.; Al-Mobark, N.M. Vulnerability assessment of the impact of sea level rise and land subsidence on north Nile delta region. *World Appl. Sci. J.* **2014**, *32*, 325–342.
6. El Sayed, M.K. Littoral and Shallow Water Deposits of the Continental Shelf Area of Egypt off Alexandria. Master's Thesis, University of Alexandria, Alexandria, Egypt, 1974; p. 150.
7. El Wakeel, S.K.; El Sayed, M.K. The texture, mineralogy, and chemistry of bottom sediments and beach sands from Alexandria region, Egypt. *Mar. Geol.* **1978**, *27*, 137–160. [[CrossRef](#)]
8. El Wakeel, S.K.; Abdou, H.F.; Mohamed, M.A. Texture and distribution of recent marine sediments of the continental shelf of the Nile Delta. *J. Geol. Soc. Iraq* **1974**, *7*, 15–34.
9. Frihy, O.E.; Iskander, M.I.; Badr, A.E. Effect of shoreline and bedrock irregularities on the morphodynamics of the Alexandria coast littoral cell, Egypt. *Geo-Mar. Lett.* **2004**, *24*, 195–211. [[CrossRef](#)]
10. Nafaa, M.E.; Frihy, O.E. Beach and nearshore features along the dissipative coastline of the Nile delta, Egypt. *J. Coast. Res.* **1993**, *9*, 423–433.
11. Misdorp, R.; Sestini, G. The Nile Delta: Main features of the continental shelf topography. In Proceedings of the Seminar on Nile Delta Sedimentology, Alexandria, Egypt, 25–29 October 1976; pp. 145–161.
12. Summerhayes, C.P.; Sestini, G.; Misdorp, R.; Marks, N. Nile delta: Nature and evolution of continental shelf sediments. *Mar. Geol.* **1978**, *27*, 43–65. [[CrossRef](#)]
13. Frihy, O.E.; Gamai, I.H. Facies analysis of Nile Delta continental shelf sediments off Egypt. *Neth. J. Sea Res.* **1991**, *27*, 165–171. [[CrossRef](#)]
14. Stanley, J.D.; Bernasconi, M.P. Relict and palimpsest depositional patterns on the Nile shelf recorded by *Mollusca faunas*. *Palaios. Res. Lett.* **1998**, *13*, 79–86. [[CrossRef](#)]
15. Toussoun, O. *Mémoires sur les Anciennes Branches du Nil, Epoque Ancienne*; Mémoire de l'Institut d'Égypte, Impr.; de l'Institut Français d'Archéologie Orientale: Le Caire, Egypt, 1922; p. 212.
16. Stanley, D.J.; Warne, A.G. Nile Delta: Recent geological evolution and human impact. *Science* **1993**, *260*, 628–634. [[CrossRef](#)] [[PubMed](#)]
17. Frihy, O.E. The Nile Delta-Patterns and processes of heavy mineral sorting and concentration. In *Heavy Minerals in Use; Development in Sedimentology 58*; Maria, A., David, T., Eds.; Elsevier: Amsterdam, The Netherlands, 2007; pp. 49–74.
18. Komar, P.D. *Beach Processes and Sedimentation*, 2nd ed.; Prentice Hall: Upper Saddle River, NJ, USA, 1998; p. 544.
19. Komar, P.D. The entrainment, transport and sorting of heavy minerals by waves and currents. In *Heavy Minerals in Use; Development in Sedimentology 58*; Maria, A., David, T., Eds.; Elsevier: Amsterdam, The Netherlands, 2007; pp. 3–48.
20. El Bouseily, A.M.; Frihy, O.E. Textural and mineralogical evidence denoting the position of the mouth of the old Canopic Nile branch on the Mediterranean coast, Egypt. *J. Afr. Earth Sci.* **1983**, *2*, 103–107. [[CrossRef](#)]
21. Fanos, A.M.; Frihy, O.E.; Khafagy, A.A.; Komar, P.D. Processes of shoreline change along the Nile Delta coast of Egypt. In Proceedings of the Coastal Sediments '91 Conference, Seattle, WA, USA, 25–27 June 1991; Volume 2, pp. 1547–1557.
22. Goldsmith, V.; Golik, A. Sediment transport model of the southeastern Mediterranean coast. *Mar. Geol.* **1980**, *37*, 146–175. [[CrossRef](#)]
23. Inman, D.L.; Jenkins, S.A. *The Nile Littoral Cell and Man's Impact on the Coastal Zone of the Southeastern Mediterranean*; Scripps Institution of Oceanography, Reference Series 84-31; University of California: La Jolla, CA, USA, 1984; p. 43.
24. Quelennec, R.E.; Manohar, M. Numerical wave refraction and computer estimation of littoral drift, application to the Nile Delta coast. In Proceedings of the Seminar on Nile Delta Coastal Processes, Alexandria, Egypt, 25–29 October 1976; UNDP/UNESCO, Academy of Scientific Research and Technology: Alexandria, Egypt, 1976; pp. 404–433.
25. Frihy, O.E.; Mohamed, S.; Abdalla, D.; El-Hattab, M. Assessment of natural coastal hazards at Alexandria/Nile Delta interface, Egypt. *Environ. Earth Sci.* **2021**, *80*, 3. [[CrossRef](#)]
26. El Fattah, T.A.; Frihy, O.E. Magnetic indications of the position of the mouth of the old Canopic branch on the northwestern Nile Delta of Egypt. *J. Coast. Res.* **1988**, *4*, 483–488.
27. Stanley, D.J.; Jorstad, T.F. Short contribution: Buried canopic channel identified near Egypt's Nile Delta Coast with radar (SRTM) imagery. *Geoarchaeology* **2006**, *21*, 503–514. [[CrossRef](#)]
28. Stanley, D.J. Nile delta margin failed and fluidized deposits concentrated along distributary channels. *Géomorphologie* **2003**, *4*, 211–226. [[CrossRef](#)]
29. Stanley, D.J.; Ullmann, T.; Athinodorou, E. Holocene Aridity-Induced interruptions of human activity along a fluvial channel in Egypt's Northern Delta. *Quaternary* **2021**, *4*, 39. [[CrossRef](#)]
30. Coutellier, V.; Stanley, D.J. Late Quaternary stratigraphy and paleogeography of the eastern Nile delta, Egypt. *Mar. Geol.* **1987**, *77*, 257–275. [[CrossRef](#)]

31. Arbouille, D.; Stanley, D.J. Late Quaternary evolution of the Burullus lagoon region, north-central Nile Delta, Egypt. *Mar. Geol.* **1991**, *99*, 45–66. [[CrossRef](#)]
32. Bruun, P. Sea level rise as a cause of shore erosion. *J. Waterw. Harb. Div.* **1962**, *88*, 117–130. [[CrossRef](#)]
33. Hallermeier, R.J. A profile zonation for seasonal sand beaches from wave climate. *Coast. Eng.* **1981**, *4*, 253–277. [[CrossRef](#)]
34. Stanley, D.J.; Addy, S.K.; Behrens, E.W. The mudline: Variability of its position relative to shelfbreak. In *The Shelfbreak: Critical Interface on Continental Margins*; Stanley, D.J., Moore, G.T., Eds.; SEPM Special Publication: Tulsa, OK, USA, 1983; Volume 33, pp. 279–298.
35. Nafaa, M.G.; Fanos, A.M.; El Ganainy, M.A. Prediction of closure depth at the Nile delta coast. *Alex. Eng. J.* **1995**, *34*, 167–173.
36. Manohar, M. Dynamic factors affecting the Nile delta coast. In Proceedings of the Seminar on Nile Delta Sedimentology, Alexandria, Egypt, 25–29 October 1976; UNDP/UNESCO, Academy of Scientific Research and Technology: Alexandria, Egypt, 1976; pp. 104–111.
37. Inman, D.L.; Elwany, M.H.; Khafagy, A.A.; Golik, A. Nile Delta profiles and migrating sand blanks. In Proceedings of the Coastal Engineering Conference, Venice, Italy, 4–9 October 1992; Volume 23, pp. 3273–3284.
38. Coleman, J.M.; Roberts, H.H.; Murlly, S.P.; Salama, M. Morphology and dynamic sedimentology of the eastern Nile delta shelf. *Mar. Geol.* **1981**, *42*, 301–326. [[CrossRef](#)]
39. Deabes, E.A.; Frihy, O.E. Estimating storm surge height in the Nile Delta coast of Egypt. In Proceedings of the First International Conference on Coastal Zone Management of River Deltas and Low Land Coastlines, Alexandria, Egypt, 6–8 March 2010; pp. 609–624.
40. Stanley, J.D.; McRea, J.E., Jr.; Waldron, J.C. *Nile Delta Drill core and Sample Database for 1985–1994: Mediterranean Basin (MEDIBA) Program*; Smithsonian Institution Press: Washington, DC, USA, 1996.
41. Stanley, J.D.; Clemente, P.L. Mica and heavy minerals as markers to map Nile Delta coastline displacements during the Holocene. *J. Coast. Res.* **2014**, *30*, 904–921. [[CrossRef](#)]
42. Shalash, S. Effect of Sedimentation on storage capacity of the High Aswan Dam reservoir. *Hydrobiologia* **1982**, *91*, 623–639. [[CrossRef](#)]
43. Bernhardt, C.E.; Horton, B.P.; Stanley, J.D. Nile Delta vegetation response to Holocene climate variability. *Geology* **2012**, *40*, 615–618. [[CrossRef](#)]
44. Stanley, J.D.; Warne, A.G. Nile Delta in its destruction phase. *J. Coast. Res.* **1998**, *14*, 794–825.
45. Stanley, J.D.; Warne, A.G.; Davis, H.R.; Bernasconi, M.P.; Chen, Z. The Late Quaternary North-Central Nile Delta from Manzala to Burullus Lagoons, Egypt. *Natl. Geogr. Res. Explor.* **1992**, *8*, 22–51.
46. Folk, R.L. *Petrology of Sedimentary Rocks*; Hemphill Pub. Co.: Austin, TX, USA, 1974; p. 182.
47. Krumbein, W.C. Size frequency distributions of sediments. *J. Sediment. Petrol.* **1934**, *4*, 65–77. [[CrossRef](#)]
48. Folk, M.; Ward, W. Brazos River Bar: Study in the significance of grain size parameters. *J. Sediment. Petrol.* **1957**, *27*, 3–26. [[CrossRef](#)]
49. Frihy, O.E.; El Sayed, E.; Deabes, E.; Gamai, I. Shelf sediments of Alexandria region, Egypt: Explorations and evaluation of offshore sand sources for beach nourishment and transport dispersion. *Mar. Georesources Geotechnol.* **2010**, *28*, 250–274. [[CrossRef](#)]
50. Tebelius, U. Bottom currents in Abu Quir Bay. In Proceedings of the Seminar on Nile Delta Sedimentology, Alexandria, Egypt, 2–9 October 1977; pp. 255–273.
51. Said, M.A. Variations of current, wind and water fluxes in the south-eastern Mediterranean off the Egyptian coast during winter and spring seasons. *Mahasagar* **1990**, *27*, 1–16.
52. Murray, S.P.; Coleman, J.M.; Roberts, H.H. Accelerated currents and sediment transport off the Damietta Nile promontory. *Nature* **1981**, *293*, 51–54. [[CrossRef](#)]
53. Flaux, C.; Morhange, C.; Marriner, N.; Rouchy, J.M. Maryout lagoon (Nile Delta, Egypt) hydrological and biosedimentary budget from 8000 to 3200 years cal. B.P. *Geomorphol. Relict Process. Environ.* **2011**, *3*, 261–278. [[CrossRef](#)]
54. Trampier, J.R. *Landscape Archaeology of the Western Nile Delta*; Lockwood Press: Bristol, CT, USA, 2014; p. 277.
55. Stoffers, P.; Summerhayes, C.P.; Dominik, J. Recent pelletoidal carbonate, sediments off Alexandria, Egypt. *Mar. Geol.* **1980**, *34*, M1–M8. [[CrossRef](#)]
56. Iskander, M.I.; Frihy, O.E.; El Ansary, A.E.; Abd El Mooty, M.M.; Nagy, N.M. Beach impacts of shore-parallel breakwaters backing offshore submerged ridges, Western Mediterranean Coast of Egypt. *J. Environ. Manag.* **2007**, *65*, 1109–1119. [[CrossRef](#)]
57. Frihy, O.E.; Dean, R. Artificial beach nourishment projects on the Egyptian coast. In Proceedings of the International Coastal Congress ICC Kiel '92, Frankfurt am Main, Germany, 7–12 September 1992; pp. 84–95.
58. El Din, S.H.S. Effect of the Aswan High Dam on the Nile flood and on the estuarine and coastal circulation pattern along the Mediterranean Egyptian coast. *Limnol. Oceanogr.* **1977**, *22*, 194–207. [[CrossRef](#)]
59. Coleman, J.M. *Deltas: Processes of Deposition and Models for Exploration*, 2nd ed.; International Human Resources Development Corp.: Boston, MA, USA, 1982; p. 124.
60. Wright, L.D. River deltas. In *Coastal Sedimentary Environments*, 3rd ed.; Davis, R.A., Ed.; Springer: New York, NY, USA, 1985; pp. 1–76.
61. Off, T. Rhythmic linear sand bodies caused by tidal currents. *Bull. Am. Assoc. Petrol. Geol.* **1963**, *47*, 324–341.
62. Kenyon, N.H. Sand ribbons European tidal seas. *Mar. Geol.* **1970**, *9*, 25–39. [[CrossRef](#)]

63. Kenyon, N.H.; Belderson, R.H. Bedforms of the Mediterranean undercurrent observed with Side-scan sonar. *Sediment. Geol.* **1973**, *9*, 77–99. [[CrossRef](#)]
64. Mamoun, M.; Ibrahim, E.M. Tectonic Activity in Egypt as indicated by earthquakes. *Helwan Inst. Astron. Geophys. Bull.* **1978**, *170*, 1–13.
65. Stanley, J.D. Subsidence in the northeastern Nile Delta: Rapid rates, possible causes, and consequences. *Science* **1988**, *240*, 497–500. [[CrossRef](#)] [[PubMed](#)]
66. Stanley, J.D. Recent subsidence and northeast tilting of the Nile delta, Egypt. *Mar. Geol.* **1990**, *94*, 147–154. [[CrossRef](#)]
67. Neev, D. The Pelusium Line—A major transcontinental shear. *Tectonophysics* **1977**, *38*, T1–T8. [[CrossRef](#)]
68. Neev, D.; Greenfield, L.; Hall, J.K. Slice tectonics in the Eastern Mediterranean Basin. In *Geological Evolution of the Mediterranean Basin*; Stanley, D., Wezel, F., Eds.; Springer: New York, NY, USA, 1985; pp. 249–269.
69. Stanley, J.D.; Clemente, P.L. Increased land subsidence and sea-level rise are submerging Egypt’s Nile Delta coastal margin. *GSA Today* **2017**, *27*, 4–11. [[CrossRef](#)]
70. Enterprise Press. Profiling the Egyptian Black Sand Company’s Burullus Plant. 2022, p. 2. Available online: <https://enterprise.press/stories/2022/10/23/profiling-the-egyptian-black-sand-companys-burullus-plant-84796/> (accessed on 3 February 2023).
71. Komar, P.D.; Li, M.Z. Beach placers at the mouth of the Columbia River, Oregon and Washington. *Mar. Min.* **1991**, *10*, 171–187.
72. Li, Z.; Komar, P.D. Longshore grain sorting and beach placer formation adjacent to the Columbia River. *J. Sediment. Petrol.* **1992**, *62*, 429–441.
73. Komar, P.D.; Wang, C. Processes of selective grain transport and the formation of placers on beaches. *J. Geol.* **1984**, *92*, 637–655. [[CrossRef](#)]
74. Sneh, A.; Weissbrod, T. Nile delta: The defunct Pelusiac branch identified. *Science* **1973**, *180*, 59–61. [[CrossRef](#)]
75. Goodfriend, G.A.; Stanley, D.G. Rapid strand-plain accretion in the northeastern Nile Delta in the 9th century A.D. and the demise of the port of Pelusium. *J. Geol.* **1999**, *27*, 147–150. [[CrossRef](#)]
76. Frihy, O.E.; Moussa, A.A.; Stanley, J.S. Abu Quir Bay, a sediment sink off the northern Nile delta, Egypt. *Mar. Geol.* **1994**, *121*, 199–211. [[CrossRef](#)]
77. El Fishawi, N.M.; Molnar, B. Nile Delta beach pebbles I: Grain size and origin. *Acta Mineral.-Petrogr. Szeged* **1981**, *26*, 25–39.
78. El Fishawi, N.M. Storms as an offshore drift agent for coarse sands, Nile Delta coast. *Acta Mineral.-Petrogr. Szeged* **1990**, *31*, 77–87.
79. DHI (Danish Hydraulic Institute). *Development of a Climate Resilient Integrated Coastal Zone Management (ICZM) Plan for the North Coast of Egypt (Numerical Wave and HD Model)*; Unpublished Report; UNDP: Hørsholm, Denmark, 2023; p. 53.
80. Stanley, J.D.; Maldonado, A. *Southeastern Mediterranean (Levantine Basin-Nile Cone) Sedimentation and Evolution*; Reports, No. 15; National Geographic Society: Washington, DC, USA, 1983; pp. 609–628.
81. Ducassou, E.; Migeon, S.; Mulder, J. and three other authors,. Evolution of the Nile deep-sea turbidite system during the late Quaternary: Influence of climate change on fan sedimentation. *Sedimentology* **2009**, *56*, 2061–2090. [[CrossRef](#)]
82. Stanley, J.D.; Corwin, K.A. Measuring strata thicknesses in cores to assess recent sediment compaction and subsidence of Egypt’s Nile delta coastal margin. *J. Coast. Res.* **2013**, *29*, 657–670. [[CrossRef](#)]
83. Goddio, F. *The Topography and Excavation of Heracleion-Thonis and East Canopus (1996–2006)*; Oxford Centre for Maritime Archaeology, Monograph 1; University of Oxford: Oxford, UK, 2007; p. 136.
84. Stanley, J.D. *Geoarchaeology, Underwater Archaeology in the Canopic Region in Egypt*; Oxford Centre for Maritime Archaeology, Monograph 2; University of Oxford: Oxford, UK, 2007; p. 128.

Disclaimer/Publisher’s Note: The statements, opinions and data contained in all publications are solely those of the individual author(s) and contributor(s) and not of MDPI and/or the editor(s). MDPI and/or the editor(s) disclaim responsibility for any injury to people or property resulting from any ideas, methods, instructions or products referred to in the content.